

## Organic Spin Clusters: Macrocyclic-Macrocyclic Polyarylmethyl Polyradicals with Very High Spin $S = 5-13$

Andrzej Rajca,\* Jirawat Wongsriratanakul, and Suchada Rajca

Contribution from the Department of Chemistry, University of Nebraska, Lincoln, Nebraska 68588-0304

Received December 5, 2003; E-mail: arajca1@unl.edu

**Abstract:** Synthesis and magnetic studies of a new class of organic spin clusters, possessing alternating connectivity of unequal spins, are described. Polyarylmethyl polyether precursors to the spin clusters, with linear and branched connectivity between calix[4]arene-based macrocycles, are prepared via modular, multistep syntheses. Their molecular connectivity and stereoisomerism are analyzed using NMR spectroscopy. The absolute masses (4–10 kDa) are determined by FABMS and GPC/MALS. Small angle neutron scattering (SANS) provides the radii of gyration of 1.2–1.8 nm. The corresponding polyradicals with 15, 22, and 36 triarylmethyls, which are prepared and studied as solutions in tetrahydrofuran- $d_6$ , may be described as  $S' = 7/2, 1/2, 7/2$  spin trimer (average  $S = 5-6$ ),  $S' = 7/2, 1/2, 6/2, 1/2, 7/2$  spin pentamer (average  $S = 7-9$ ), and spin nonamer (average  $S = 11-13$ ), respectively, as determined by SQUID magnetometry and numerical fits to linear combinations of the Brillouin functions. For spin trimer and pentamer, the quantitative magnetization data are fit to new percolation models, based upon random distributions of chemical defects and ferromagnetic vs antiferromagnetic couplings. The value of  $S = 13$  is the highest for an organic molecule.

### 1. Introduction

Dendritic-macrocyclic polyradical **1** is designed as an “organic spin cluster” (Figure 1).<sup>1,2</sup> Its average value of spin quantum number,  $S \approx 10$ , in the ground state, is the highest among organic molecules.<sup>2-12</sup> However, both the average value of  $S$  and average number of unpaired electrons in **1** are below the expected values for a polyradical with 24 ferromagnetically coupled electron spins.<sup>1</sup> There are two key problems to consider: chemical defects (incomplete generation of unpaired electrons) and antiferromagnetic couplings (caused by out-of-plane twisting of the  $\pi$  system).<sup>3,13-21</sup>

In **1**, one chemical defect at any of the four 4-biphenyl-substituted triarylmethyl sites in the dendritic branches would disrupt the exchange coupling and drastically lower the overall value of  $S$ . Furthermore, the component spins ( $S'$ ) for the branch ( $S' = 5/2$ ) and the core ( $S' = 4/2$ ) have similar values (Figure 1); thus, if their exchange coupling is reversed from ferromagnetic-to-antiferromagnetic, as a result of the out-of plane twisting at one of the biphenyl moieties, both average value of  $S$  and average number of unpaired electrons are drastically lowered.<sup>1,3</sup>

One approach to counter this problem is to replace the dendritic branches with macrocyclic branches, to minimize the impact of chemical defects.<sup>13,15</sup> However, sterically large macrocyclic branches may introduce problems with both synthesis and exchange coupling (through severe out-of-plane twisting). The use of a relatively long linker, such as bis(biphenylene)-methyl, for connecting the branch to the core may alleviate these problems. Implementation of this design leads to a new class of “organic spin clusters”,<sup>22-24</sup> possessing alternating connectivity of unequal spins, as illustrated by polyradicals **2** (spin trimer), **3** (spin pentamer), and **4** (spin nonamer) (Figure 2).<sup>3</sup>

- (1) Rajca, S.; Rajca, A.; Wongsriratanakul, J.; Butler, P.; Choi, S. *J. Am. Chem. Soc.* **2004**, *126*, in press.
- (2) Rajca, A.; Wongsriratanakul, J.; Rajca, S.; Cerny, R. *Angew. Chem. Int. Ed.* **1998**, *37*, 1229–1232.
- (3) Rajca, A. *Chem. Eur. J.* **2002**, *8*, 4834–4841.
- (4) Itoh, K.; Kinoshita, M., Eds.; *Molecular Magnetism*; Gordon and Breach: Kodansha, 2000; pp 1–337.
- (5) Lahti, P. M., Ed. *Magnetic Properties of Organic Materials*; Marcel Dekker: New York, 1999; pp 1–713.
- (6) Crayston, J. A.; Devine, J. N.; Walton, J. C. *Tetrahedron* **2000**, *56*, 7829–7857.
- (7) Rajca, A.; Wongsriratanakul, J.; Rajca, S. *Science* **2001**, *294*, 1503–1505.
- (8) Rajca, A.; Rajca, S.; Wongsriratanakul, J. *J. Am. Chem. Soc.* **1999**, *121*, 6308–6309.
- (9) Iwamura, H.; Koga, N. *Acc. Chem. Res.* **1993**, *26*, 346–351.
- (10) Matsuda, K.; Nakamura, N.; Inoue, K.; Koga, N.; Iwamura, H. *Bull. Chem. Soc. Jpn.* **1996**, *69*, 1483–1494.
- (11) Nishide, H.; Ozawa, T.; Miyasaka, M.; Tsuchida, E. *J. Am. Chem. Soc.* **2001**, *123*, 5942–5946.
- (12) Michinobu, T.; Inui, J.; Nishide, H. *Org. Lett.* **2003**, *5*, 2165–2168.
- (13) Rajca, A. *Chem. Rev.* **1994**, *94*, 871–893.
- (14) Rajca, A.; Utamapanya, S. *J. Am. Chem. Soc.* **1993**, *115*, 10688–10694.
- (15) Rajca, A.; Rajca, S.; Padmakumar, R. *Angew. Chem., Int. Ed. Engl.* **1994**, *33*, 2091–2093.
- (16) Dvolaitzky, M.; Chiarelli, R.; Rassat, A. *Angew. Chem., Int. Ed. Engl.* **1992**, *31*, 180–181.

- (17) Silverman, S. K.; Dougherty, D. A. *J. Phys. Chem.* **1993**, *97*, 13273–13283.
- (18) Kanno, F.; Inoue, K.; Koga, N.; Iwamura, H. *J. Am. Chem. Soc.* **1993**, *115*, 847–850.
- (19) Fang, S.; Lee, M.-S.; Hrovat, D. A.; Borden, W. A. *J. Am. Chem. Soc.* **1995**, *117*, 6727–6731.
- (20) Rajca, A.; Rajca, S. *J. Chem. Soc., Perkin 2* **1998**, 1077–1082.
- (21) Shultz, D. A.; Fico, R. M., Jr.; Bodnar, S. H.; Kumar, K.; Vostrikova, K. E.; Kampf, J. W.; Boyle, P. D. *J. Am. Chem. Soc.* **2003**, *125*, 11761–11771.
- (22) Rajca, A.; Rajca, S. *J. Am. Chem. Soc.* **1996**, *118*, 8121–8126.
- (23) Rajca, A.; Wongsriratanakul, J.; Rajca, S. *J. Am. Chem. Soc.* **1997**, *119*, 11674–11686.
- (24) Rajca, A. *Mol. Cryst. Liq. Cryst.* **1997**, *305*, 567–577.

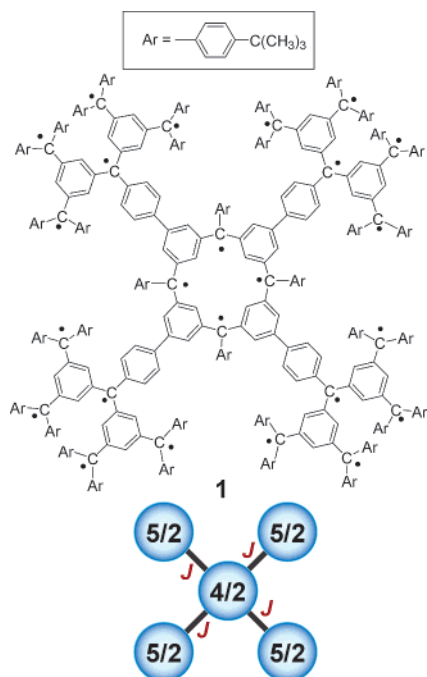


**Figure 1.** Dendritic-macrocylic polyradical **1** ( $S \approx 10$ ) as spin pentamer.

Overall design of polyradicals **2**, **3**, and **4** is based upon  $S \gg 1/2$  macrocyclic modules connected with  $S = 1/2$  bis(biphenylene)methyl linkers. Such alternating connectivity of unequal spins is expected to address out-of-plane twistings, which may reverse the sign of exchange coupling from ferromagnetic to antiferromagnetic. For example, pentadecaradical **2** may be viewed as a quasilinear trimer of unequal spins,  $S_1 - 1/2 - S_1$ , where  $S_1 = 7/2$  (Figures 2 and 3). The reversal of both ferromagnetic couplings to antiferromagnetic ones would lower the overall value of  $S$  from  $2S_1 + 1/2$  to  $2S_1 - 1/2$ , i.e., only by one unit. The limited cancellation of spins is expected to exist for random distribution of ferromagnetic and antiferromagnetic couplings as well. This is in contrast to **1**, in which directly connected spins are approximately equal, e.g.,  $S' = 5/2$  and  $S'' = 4/2$  in **1** (Figure 1).

The design, based upon partial cancellation of unequal spins through antiferromagnetic coupling, corresponds to a “ferrimagnetic coupling scheme”, which is widely applied to organometallic ferrimagnets.<sup>25,26</sup> Examples are coordination polymers and networks of nitroxides, e.g., antiferromagnetic couplings of  $S = 5/2$   $\text{Mn}^{\text{II}}$  with  $S = 1/2$  nitronyl nitroxides or  $S = 1$  dinitroxides (or  $S = 3/2$  trinitroxides).<sup>27,28</sup> Examples of organic radicals (carbenes), which are intended for such partial cancellation of spins, give relatively values of  $S = 1$  only.<sup>29</sup>

Polyradicals **2–4** may also be viewed as linear and branched fragments of the first conjugated polymer with magnetic ordering.<sup>7,8</sup> Analysis of magnetic data for such model molecules

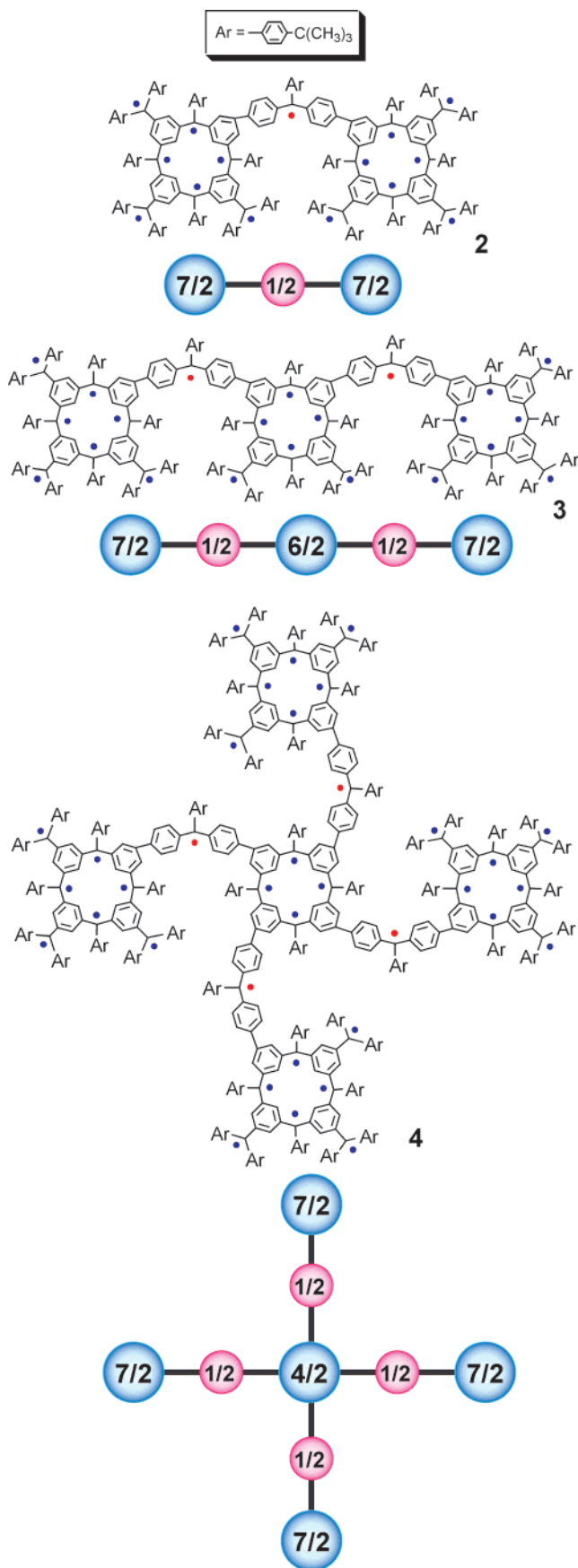


**Figure 2.** Macrocyclic-macrocylic polyradicals **2**, **3**, and **4** as organic spin clusters.

- (25) (a) Manriquez, J. M.; Yee, G. T.; McLean, R. S.; Epstein, A. J.; Miller, J. S. *Science* **1991**, *252*, 1415–1417. (b) Holmes, S. M.; Girolami, G. S. *J. Am. Chem. Soc.* **1999**, *121*, 5593–5594.
- (26) For progress in organic ferrimagnets, see: (a) Buchanenko, A. L. *Russ. Chem. Rev.* **1990**, *59*, 307–319. (b) Hosokoshi, Y.; Katoh, K.; Nakazawa, Y.; Nakano, H.; Inoue, K. *J. Am. Chem. Soc.* **2001**, *123*, 7921–7922. (c) Shiomi, D.; Kanaya, T.; Sato, K.; Mito, M.; Takeda, K.; Takui, T. *J. Am. Chem. Soc.* **2001**, *123*, 11823–11824.
- (27) Caneschi, A.; Gatteschi, D.; Rey, P. *Prog. Inorg. Chem.* **1991**, *39*, 331–429.
- (28) Iwamura, H.; Inoue, K.; Koga, N. *New J. Chem.* **1998**, 201–210.
- (29) Tricarbene with triplet ground state: Itoh, K.; Takui, T.; Teki, Y.; Kinoshita, T. *Mol. Cryst. Liq. Cryst.* **1989**, *176*, 49–66.

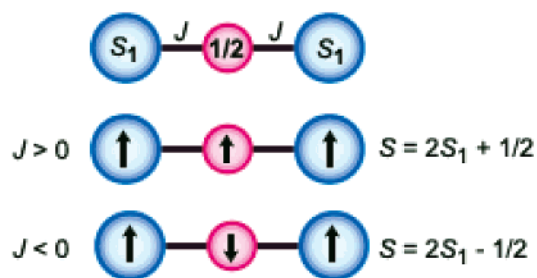


Figure 3. Alternating connectivity of unequal spins in pentadecaradical 2.

may provide a rationale for extraordinary extent of net ferromagnetic exchange couplings leading to high values of magnetic moment (or  $S$ ) in such polymers.<sup>30</sup>

This article describes the synthesis and characterization of a novel series of high-spin polyradicals **2**, **3**, and **4** with 15, 22, and 36 triarylmethyls, respectively (Figure 2). Their corresponding average values of  $S$  are 5–6, 7–9, and 11–13. The  $S = 13$  is a new record for an organic molecule.

## 2. Results and Discussion

**2.1. Synthesis of Polyethers.** Modular and convergent synthesis is used to prepare polyethers **2**-(OMe)<sub>15</sub>, **3**-(OMe)<sub>22</sub>, and **4**-(OMe)<sub>36</sub>. The synthesis is carried out in three stages: (1) preparation of 1,3-phenylene-connected macrocyclic monofunctionalized modules, (2) attachment of linkers to the monofunctionalized modules (“modules-with-linkers”), and (3) attachment of monofunctionalized modules-with-linkers to macrocyclic cores, forming bis(biphenylene)methyl moieties (Schemes 1 and 2).

**2.1.1. Macrocyclic Monofunctionalized Modules 11.** 5-Bromo-1,3-dilithiobenzene,<sup>31</sup> prepared by double Br/Li exchanges from 1,3,5-tribromobenzene, is treated with 1-(4-*tert*-butylbenzoyl)-pyrrolidine to give diketone **5** (Scheme 1). Analogously, ketone **7** is obtained from 1,3-dibromoaryl compound **6**,<sup>15</sup> via mono Br/Li exchange. Double Br/Li exchange on **6**, using *t*-BuLi (4.2 equiv) in ether, is followed with addition of ketone **7** (2.4 equiv); the resultant diol **8** is obtained as a mixture (1:0.4–1:0.9) of two diastereomers in 46–51% yields. Diol **8** is converted to dibromopentaether **9** in 67–90% yield using NaH in THF. The macrocyclic ring of calix[4]arene is constructed through the addition of the bis(aryllithiums) to diketones.<sup>1,32,33</sup> In the present synthesis, the bis(aryllithiums) are generated in situ from a mixture of diastereomers dibromopentaether **9** and then condensed with diketone **5**; final concentrations of **5** and **9** are 0.006 M. Three *cis/trans* isomers of pentaether-diols **10A–10C** are isolated in 5–12% yields (19–24% overall yields). Etherification gives the corresponding heptaethers (modules) **11A–11C** in moderate yields. Also, a small amount of heptaether **11D** is isolated from the reaction mixture containing **11A**.

Assuming fast conformational exchange, six *cis/trans* isomers are possible for both pentaether-diols **10** and heptaethers **11**;

these are two  $C_s$ -, two  $C_2$ -, and two  $C_1$ -symmetric isomers (Figure 4).

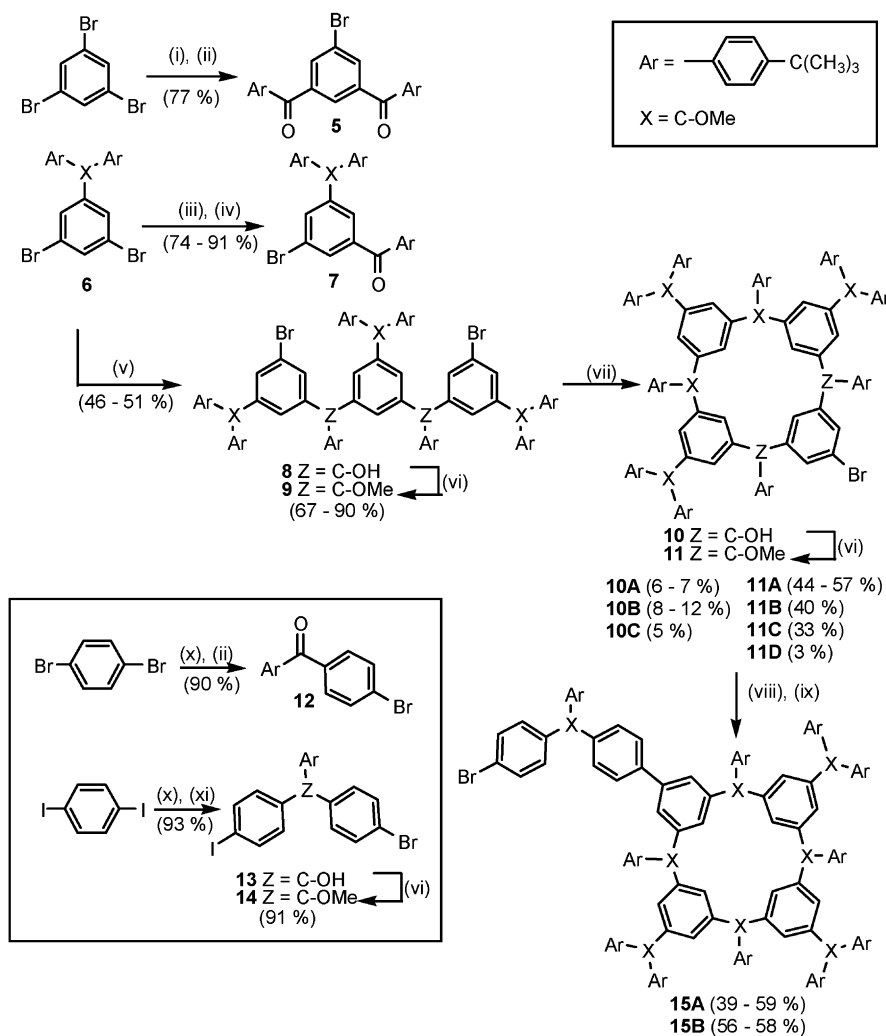
Only three major isomers are isolated for each macrocycle:  $C_s$ -symmetric **10A** (and **11A**) and two  $C_1$ -symmetric **10B** and **10C** (**11B** and **11C**). Also, a small amount of  $C_2$ -symmetric heptaether **11D** is obtained. For each isomer, FABMS gives the expected  $(M - OCH_3)^+$  isotopic cluster ions; the pentaether-diols **10** show additional, intense  $(M - OH)^+$  isotopic cluster ions. Measured and calculated isotopic distributions for both cluster ions show satisfactory agreement. The presence of the OH groups in pentaether-diols (**10A–10C**) is corroborated by the IR absorptions in the 3400–3600  $\text{cm}^{-1}$  range and the D<sub>2</sub>O exchange experiments using <sup>1</sup>H NMR spectroscopy. The <sup>1</sup>H and <sup>13</sup>C NMR spectra (Tables 1s–4s, Supporting Information) show reasonable agreement (less a few spectral overlaps) between the expected and observed number of resonances. Although the point groups of symmetry are determined, the two possible structures within the same point group of symmetry are indistinguishable by standard NMR spectroscopy.<sup>34</sup> For the  $C_s$ -symmetric isomer, NMR spectra are best interpreted in terms of five nonequivalent sets of two 4-*tert*-butylphenyl groups; the four 1,3,5-trisubstituted benzene rings appear as a pair of equivalent rings and a pair of nonequivalent rings. The NMR spectra for the  $C_2$ -symmetric **11D** are similar to the  $C_s$ -symmetric **11A**, except for one diastereotopic pair of 4-*tert*-butylphenyl groups in **11D**, as expected for this chiral isomer.<sup>35</sup> <sup>1</sup>H chemical shifts for the diastereotopic 4-*tert*-butylphenyl groups are significantly different ( $\Delta\delta = 0.012$ – $0.064$  ppm) in both aromatic (7.478 and 7.182 vs 7.414 and 7.194 ppm) and *tert*-butyl (1.196 vs 1.146 ppm) regions. For each  $C_1$ -symmetric isomer (**11B** and **11C**), 10 nonequivalent 4-*tert*-butylphenyl groups and four nonequivalent 1,3,5-trisubstituted benzene rings are found, as expected.

**2.1.2. Modules-with-Linkers 15.** Linker **14** is prepared from 1,4-dibromobenzene and 1,4-diiodobenzene in 76% overall yield (Scheme 1). Negishi coupling is employed to connect racemic linker **14** to the macrocyclic modules (achiral **11A** and racemic **11B**) providing modules-with-linkers **15A** and **15B** in about 50% isolated yields (Scheme 1).<sup>36</sup> **15A** and **15B** are isolated as racemate and a ~1:1 mixture of diastereomers, respectively. In FABMS, the expected  $(M - OCH_3)^+$  isotopic cluster ions have dominant intensity in the  $m/z = 480$ – $3000$  range. The assignments of NMR spectra for **15A** and **15B** (Figures 1s and 2s and Table 5s, Supporting Information, and Figures 5 and 6) are discussed in the following paragraphs.

For **15A**, six singlets (1:1:1:1:2:2) are found in the methoxy group region of the <sup>1</sup>H NMR (500 MHz, 293 K) spectrum,

- (30) (a) The design annelated macrocyclic organic spin clusters, addressing the dimensionality of the conjugated polymer with magnetic ordering, is described in Rajca, A.; Wongsriratanakul, J.; Rajca, S.; Cerny, R. L. *Chem. Eur. J.* **2004**, *10*, in press. (b) The possible role of magnetic shape anisotropy in the conjugated polymer with magnetic ordering is addressed in ref 1.
- (31) Bromo-1,3-dilithiobenzene: Rot, N.; Bickelhaupt, F. *Organometallics* **1997**, *16*, 5027–5031.
- (32) Rajca, A.; Padmakumar, R.; Smithhisler, D. J.; Desai, S. R.; Ross, C. R.; Stezowski, J. J. *J. Org. Chem.* **1994**, *59*, 7701–7703.
- (33) Rajca, A.; Rajca, S.; Desai, S. R. *J. Am. Chem. Soc.* **1995**, *117*, 806–816.

- (34) Crystals of adequate quality for single-crystal X-ray diffraction could not be obtained for **11A–11D**. Structures of the  $C_s$ - and  $C_2$ -symmetric isomers (**11A** and **11D**) could in principle be determined via laborious chemical transformation to more symmetric compounds, such as octaethers.<sup>15</sup> Point groups of symmetry for such octaethers are analogous to the isomers of tetrabromo-calix[4]arene core **18** in ref 1. The  $C_s$ -symmetric isomers are expected to give octaethers with  $C_{4v}$  and  $C_{2h}$  point groups; similarly, the  $C_2$ -symmetric isomers are expected to give octaethers with  $D_{2d}$  and  $C_{2h}$  point groups. In both cases, the octaethers are distinguishable by NMR spectroscopy. This procedure would fail for the  $C_1$ -symmetric isomers because both isomers of the corresponding octaethers possess a  $C_s$  point group.
- (35) The experiments with the mixed chiral shift agent, such as Ag(fod) and ytterbium tris[3-heptafluoropropylhydroxymethylene-(+)-camphorate (Yb(hpfc)), and **11D** in chloroform-*d* (with **11A** as reference) were not successful, that is, there was no detectable change in the <sup>1</sup>H NMR spectral patterns (no additional splittings) for the  $C_2$ -symmetric **11D**.
- (36) Negishi, E.; King, A. O.; Okukado, N. *J. Org. Chem.* **1977**, *42*, 1821–1823.

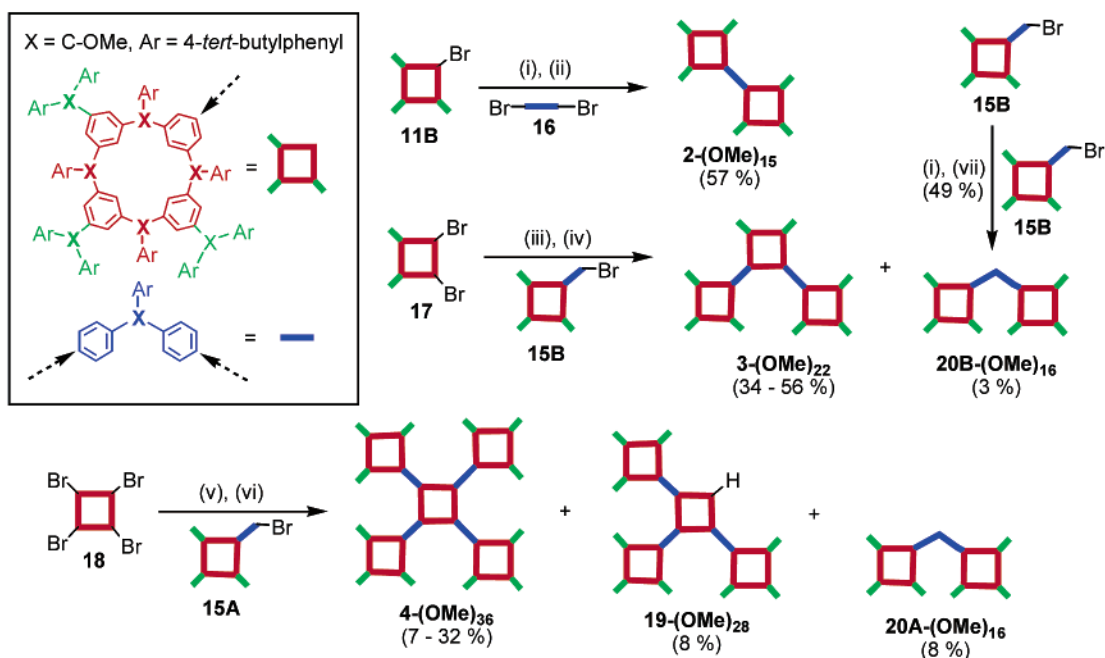
**Scheme 1.** Synthesis of Modules **11**, Linker **14**, and Modules-with-Linkers **15**<sup>a</sup>

<sup>a</sup> Conditions: (i) *t*-BuLi (4 equiv), ether,  $-78\text{ }^{\circ}\text{C}$  for 1.5 h; (ii) 1-(4-*tert*-butylbenzoyl)pyrrolidine as solid,  $-78\text{ }^{\circ}\text{C}$  to room temperature for 1 d; (iii) *t*-BuLi (2 equiv), THF,  $-78\text{ }^{\circ}\text{C}$  for 3.5 h; (iv) 1-(4-*tert*-butylbenzoyl)pyrrolidine as 0.5 M solution in THF,  $-78\text{ }^{\circ}\text{C}$  to room temperature for 12 h; (v) *t*-BuLi (4.2 equiv), ether,  $-78\text{ }^{\circ}\text{C}$  for 2 h, then  $-20\text{ }^{\circ}\text{C}$  for 30 min, then **7** (2.2 equiv),  $-78\text{ }^{\circ}\text{C}$  to room temperature for 2.5 d; (vi) NaH (3–11 equiv), THF, then indicated diols **8**, **10A–10C**, or alcohol **13**,  $0\text{ }^{\circ}\text{C}$  to room temperature for 3 h, then MeI (8–18 equiv),  $0\text{ }^{\circ}\text{C}$  to room temperature for 1 d; (vii) **9** (0.009 M in THF), then *t*-BuLi (4.0 equiv),  $-78\text{ }^{\circ}\text{C}$  for 2.5 h, then  $-20\text{ }^{\circ}\text{C}$  for 15 min, then **5** (1.0 equiv, 0.02 M in THF),  $-78\text{ }^{\circ}\text{C}$  to room temperature for 1 d; (viii) *t*-BuLi (2.1–2.2 equiv), THF,  $-78\text{ }^{\circ}\text{C}$  for 3 h, then  $-20\text{ }^{\circ}\text{C}$  for 10 min, then ZnCl<sub>2</sub> (1.1–1.2 equiv),  $-78\text{ }^{\circ}\text{C}$  to room temperature for 3–5 h; (ix) **14** (2.0 equiv), then Pd(PPh<sub>3</sub>)<sub>4</sub> (3 mol %),  $100\text{ }^{\circ}\text{C}$ , 1.5 d; (x) *n*-BuLi (1.0 equiv), ether,  $-78\text{ }^{\circ}\text{C}$  for 2 h; (xi) **12**,  $-78\text{ }^{\circ}\text{C}$  to room temperature for 1 d, then I<sub>2</sub> (0.10 equiv). Stereoisomers **11C** and **11D** are not analytically pure.

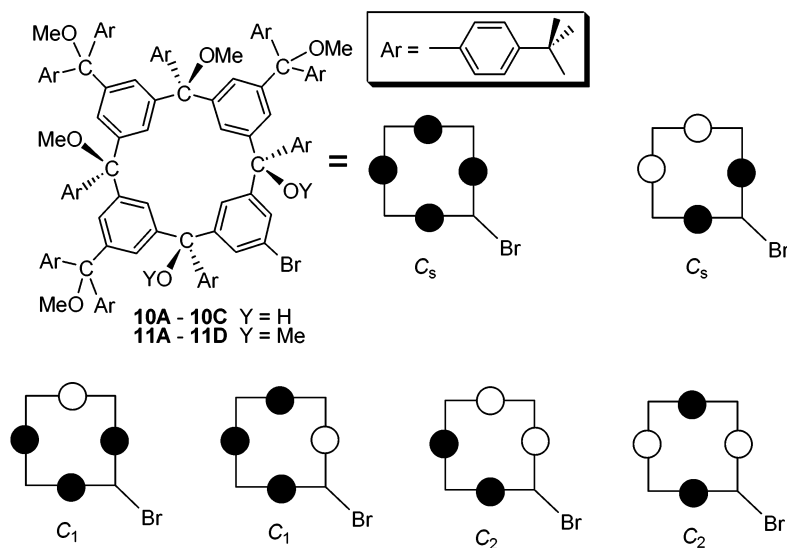
suggesting that at least one pair of methoxy groups is diastereotopic. In the aromatic region, four types of benzene rings (color-coded in Figure 5) are assigned, on the basis of the <sup>1</sup>H–<sup>1</sup>H COSY spectrum, spectral patterns, and relative integrations. The pair of 1,3,5-trisubstituted benzene rings (rings A and A', Figure 5), which is equivalent in the C<sub>s</sub>-symmetric **11A**, is now diastereotopic, showing as two pairs of nearly coincident ( $\Delta\delta \approx 0.003\text{ ppm}$ ) 1-proton triplets ( $J = 2\text{ Hz}$ ) and one 2-proton triplet ( $J = 2\text{ Hz}$ ). The other nonequivalent pair of 1,3,5-trisubstituted benzene rings (rings B and C, Figure 5) still appears as two sets of three 1-proton triplets with  $J = 2\text{ Hz}$  (Figure 1s, Supporting Information). Ten 4-proton doublets ( $J = 8\text{--}9\text{ Hz}$ ), with pairwise correlations in the COSY spectrum, may correspond to two sets of five 1,4-disubstituted benzene rings (rings 1–5 and 1'–5', Figure 5); although the two sets should be diastereotopic, the chemical shift differences may not be detectable. Four 2-proton doublets ( $J = 8\text{--}9\text{ Hz}$ ) and the 4-proton singlet at 7.247 ppm may be assigned to the remaining

1,4-disubstituted benzene rings (rings 6–8, Figure 5). Overall, the <sup>1</sup>H NMR spectra for **15A** largely reflect the 2-fold symmetry of the macrocyclic module **11A**, except for the very few resolvable, small diastereotopic splittings.

For **15B**, eight resonances (three protons each) are found in the methoxy group region of the <sup>1</sup>H NMR (500 MHz, 293 K) spectrum; however, five of those resonances are further split ( $\Delta\delta \approx 0.001\text{--}0.003\text{ ppm}$ ) into two singlets each (with approximately equal peak height). In the aromatic region, two types of benzene rings (color-coded in Figure 6) are assigned, on the basis of <sup>1</sup>H–<sup>1</sup>H COSY spectrum, spectral patterns, and relative integrations. For the 1,3,5-trisubstituted benzene rings (rings A–D, Figure 6), majority of the 12 1-proton resonances are either appearing as two triplets ( $\Delta\delta \approx 0.003\text{ ppm}$ ) or are broadened, unlike well-defined triplets for **11B** (Figure 2s, Supporting Information). These additional splittings are less noticeable in the more spectrally overlapped region of 1,4-disubstituted benzene rings (rings 1–13, Figure 6). In this

**Scheme 2.** Synthesis of Polyethers 2-(OMe)<sub>15</sub>, 3-(OMe)<sub>22</sub>, and 4-(OMe)<sub>36</sub><sup>a</sup>

<sup>a</sup> (i) *t*-BuLi (2.1–2.2 equiv), THF, –78 °C for 3–4 h, then –20 °C for 10 min, then ZnCl<sub>2</sub> (1.1–1.2 equiv), –78 °C to room temperature for 3 h; (ii) **16** (0.5 equiv), then Pd(PPh<sub>3</sub>)<sub>4</sub> (3 mol %), 100 °C, 1.5 d; (iii) *t*-BuLi (5 equiv), THF, –78 °C for 2 h, then –20 °C for 10 min, then ZnCl<sub>2</sub> (4.5 equiv), –78 °C to room temperature for 3–5 h; (iv) **15B** (~3 equiv), then Pd(PPh<sub>3</sub>)<sub>4</sub> (4 mol %), 100 °C, 3 d; (v) *t*-BuLi (10 equiv), THF, –78 °C for 2 h, then –20 °C for 10 min, then ZnCl<sub>2</sub> (~5 equiv), –78 °C to room temperature for ~5 h; (vi) **15A** (~6 equiv), then Pd(PPh<sub>3</sub>)<sub>4</sub> (10 mol %), 100 °C, 2–3 d; (vii) **15B** (1 equiv), then Pd(PPh<sub>3</sub>)<sub>4</sub> (2 mol %), 100 °C, 1 d.

**Figure 4.** Possible *cis/trans* isomers of diols **10** and modules **11**. Open and closed circles correspond to the relative orientation of the OMe (and OH) groups.

region, 24 2-proton doublets ( $J = 8\text{--}9$  Hz), which are correlated pairwise in the COSY spectrum, account for 12 1,4-disubstituted benzene rings. However, the 13th ring appears as two 1-proton singlets and one 2-proton singlet (all within 0.007 ppm), i.e., two overlapped AB systems. In the aromatic region of the <sup>13</sup>C NMR spectra, 46 resonances are resolved vs the expected 38 for quaternary carbons; in particular, two resonances at 121.62 and 121.60 ppm for C–Br group are found. These observations suggest that **15B** is isolated as nearly equimolar mixture of two diastereomers, which possess nearly identical chemical shifts.

**2.1.3. Polyethers 2-(OMe)<sub>15</sub>, 3-(OMe)<sub>22</sub>, and 4-(OMe)<sub>36</sub>.** Negishi coupling is employed to form the target polyethers, forming bis(biphenylene)methyl moieties (Scheme 2).<sup>36</sup>

Pentadecaether **2-(OMe)<sub>15</sub>** is obtained via condensation of module **11B** and symmetrical linker **16**; the target pentadecaether is isolated as two fractions, both mixtures of diastereomers, in 57% overall yield. Because *C*<sub>1</sub>-symmetric **11B** is used as a racemic mixture and a pseudoasymmetric center is formed, three diastereomers are possible for **2-(OMe)<sub>15</sub>**, i.e., one pair of enantiomers and two *meso* compounds.

Condensation of the module-with-linker **15B** (3 equiv, two diastereomers) with *C*<sub>1</sub>-symmetric dibromo-calix[4]arene core **17** (1 equiv) gives docosaether (22-ether) **3-(OMe)<sub>22</sub>** as a mixture of diastereomers in 34% and 56% yields.<sup>37,38</sup> As **15B**

(37) Rajca, A.; Lu, K.; Rajca, S. *J. Am. Chem. Soc.* **1997**, *119*, 10335–10345.

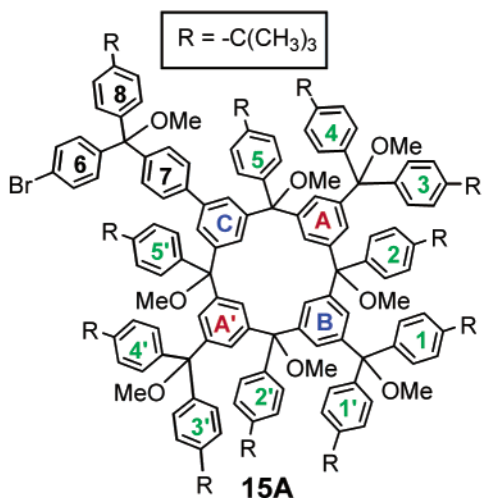


**Figure 5.** Module-with-linker **15A** with numbering scheme for the assignment of  $^1\text{H}$  NMR spectra.

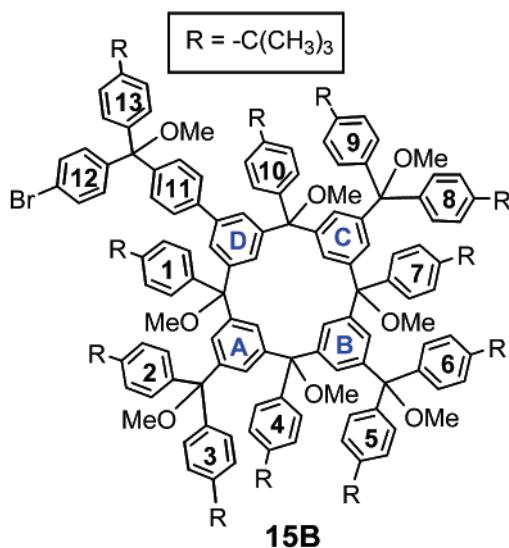


**Figure 6.** Module-with-linker **15B** with numbering scheme for the assignment of NMR spectra.

is an approximately equimolar mixture of  $C_1$ -symmetric diastereomers and  $C_1$ -symmetric **17** is racemic, the product **3-(OMe)<sub>22</sub>** possesses five distinct chiral elements; therefore, a complex mixture of diastereomers is possible.

Similarly, hexatriacontaeether (36-ether) **4-(OMe)<sub>36</sub>** is obtained in 7–32% yields from racemic module-with-linker **15A** (5–6 equiv) and  $C_{4v}$ -symmetric tetrabromo-calix[4]arene core **18**.<sup>39</sup> Because racemic **15A** and achiral  $C_{4v}$ -symmetric **18** are used in the synthesis of 36-ether **4-(OMe)<sub>36</sub>**, the four constitutionally identical and circularly disposed chiral centers in **4-(OMe)<sub>36</sub>** should lead to a mixture of diastereomers (two pairs of enantiomers and two *meso* compounds).<sup>40</sup>

In the synthesis of 22-ether **3-(OMe)<sub>22</sub>**, the side product **20B-(OMe)<sub>16</sub>**, corresponding to the homocoupling product of the modules-with-linker **15B**, is isolated in 3% yield. Direct Negishi

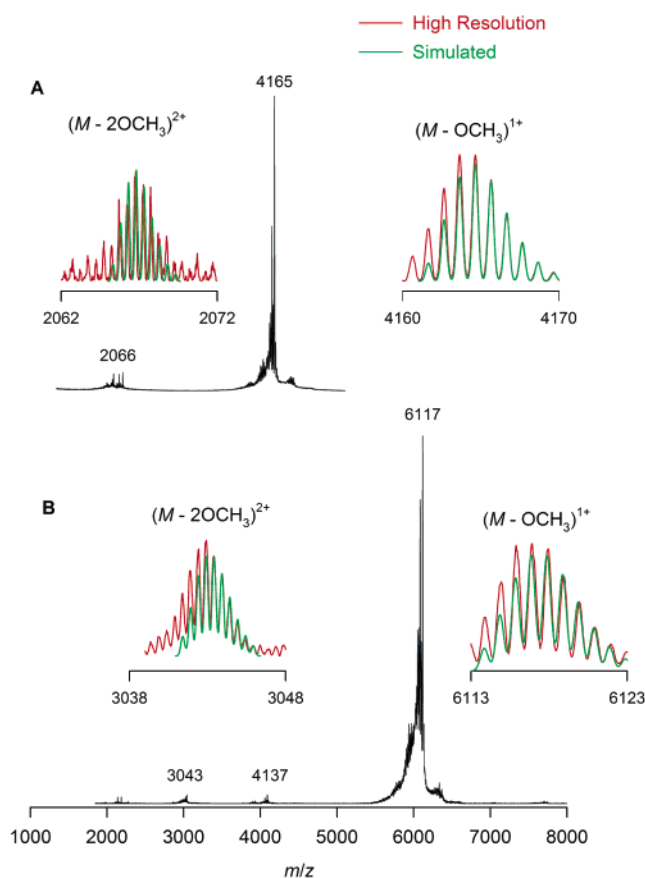


**Figure 7.** FABMS (ONPOE) for pentadecaether **2-(OMe)<sub>15</sub>** (plot A) and 22-ether **3-(OMe)<sub>22</sub>** (plot B). Main plots: low-resolution spectra. Inset plots: high-resolution spectra (red lines) and simulations of the isotopic intensities at natural isotopic abundance (green lines) for the  $(M - \text{OCH}_3)^+$  and  $(M - 2\text{OCH}_3)^{2+}$  ion clusters.

coupling of **15B** gives the product (49% yield) with FABMS and  $^1\text{H}$  NMR data identical to that for **20B-(OMe)<sub>16</sub>** (Scheme 2).<sup>41</sup>

In the synthesis of 36-ether **4-(OMe)<sub>36</sub>**, the side products **19-(OMe)<sub>28</sub>** and **20A-(OMe)<sub>16</sub>** are isolated in 8% and 8.5% yields, respectively (Scheme 2). The target 36-ether **4-(OMe)<sub>36</sub>** and side product **19-(OMe)<sub>28</sub>** are difficult to separate by chromatography on silica, as a result of not only the overlapping  $R_f$  values but also low recovery of the polyethers. Presumably, the polyethers are slowly demethylated upon contact with silica, especially with activated silica.<sup>42</sup> For example, small amounts of monodemethylation products of **20A-(OMe)<sub>16</sub>** (labeled as **20A-(OMe)<sub>15</sub>OH**), which are identified in selected samples of both **4-(OMe)<sub>36</sub>** and **19-(OMe)<sub>28</sub>** by FABMS (Figure 8).

**2.1.3.A. FABMS of Target Polyethers and Their Side Products.** FABMS for the target polyethers **2-(OMe)<sub>15</sub>**, **3-(OMe)<sub>22</sub>**, and **4-(OMe)<sub>36</sub>** show intense  $(M - \text{OCH}_3)^+$  ions. The isotopic intensities are resolved for both singly and doubly charged ions in **2-(OMe)<sub>15</sub>** and **3-(OMe)<sub>22</sub>**; only broadened, average mass peaks are found for **4-(OMe)<sub>36</sub>** (Figures 7 and 8).

Both fractions of pentadecaether **2-(OMe)<sub>15</sub>** give indistinguishable low-resolution FABMS in the  $m/z$  1000–5000 range,

(38) The  $C_1$ -symmetric **17** corresponds to the least polar *cis/trans* isomer **7A** in ref 37.

(39) Synthesis and characterization of the  $C_{4v}$ -symmetric tetrabromo-calix[4]-arene core **18** is described in refs 1 and 2.

(40) For other examples of cyclostereoisomerism, see: Eliel, E. L.; Wilen, S. H. *Stereochemistry of Organic Compounds*; Wiley: New York, 1994, 1176–1177.

(41) The  $^1\text{H}$  chemical shifts for both products are within 0.01 ppm at room temperature.

(42) Our previous attempts to separate polyarylmethyl polyethers using either normal or reverse phase HPLC have not been successful. For selected chromatographic separations, silica is activated at 200 °C.

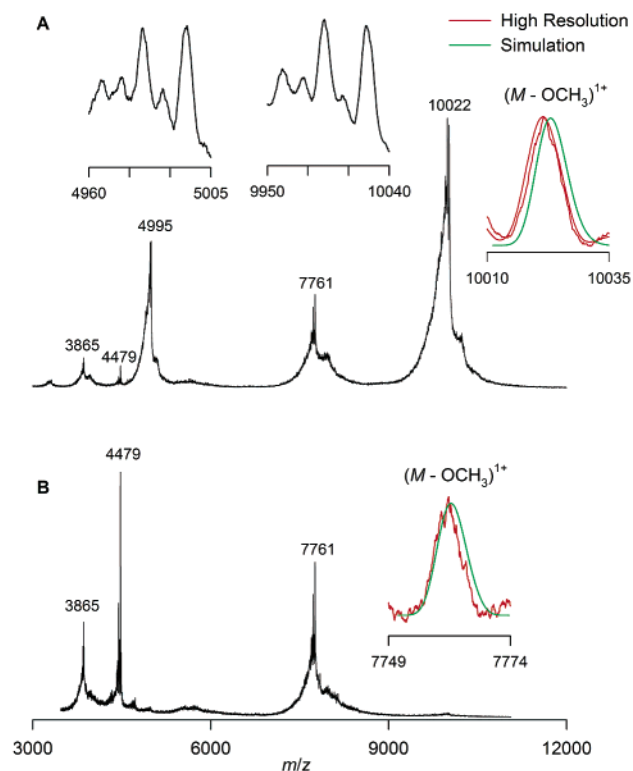


**Figure 8.** FABMS (ONPOE) for 36-ether **3-(OMe)<sub>36</sub>** (plot A) and side product **19-(OMe)<sub>28</sub>** (plot B). Main plots: low-resolution spectra. Inset plots: fragmentation patterns for the  $m/z$  10022 and  $m/z$  4995 peaks of **3-(OMe)<sub>36</sub>** (black lines), and high-resolution spectra (red lines) and simulations of the isotopic intensities at natural isotopic abundance (green lines) for the  $(M - \text{OCH}_3)^+$  ion clusters.

showing the dominant peak at  $m/z$  4165. The high-resolution spectrum reveals an isotopic cluster ion, which matches well with the calculated spectrum for the singly charged  $(M - \text{OCH}_3)^+$  ion, except for the small extra intensity on the side of the lower  $m/z$  (Figure 7A). Additional small peaks (<10% relative amplitude) are found in the  $m/z$  2060–2190 region. The high-resolution spectrum show a doubly charged isotopic cluster ion at  $m/z$  2066 (spacing of  $m/z$  0.5 for isotopic peaks) for the  $(M - 2\text{OCH}_3)^{2+}$  ion. Also, singly charged cluster at  $m/z$  2185 for the  $(M - \text{C}_{144}\text{H}_{167}\text{O}_7)^+$  ion is found; this ion corresponds to the loss of “macroyclic module with benzene ring”, with the possible formation of a relatively stable  $\alpha$ -methoxybenzhydryl cation.

For 22-ether **3-(OMe)<sub>22</sub>**, the low-resolution FABMS shows the dominant peak at  $m/z$  6117; the high-resolution spectrum gives an isotopic cluster in satisfactory agreement with the calculated spectrum for the singly charged  $(M - \text{OCH}_3)^+$  ion, i.e.,  $\text{C}_{439}\text{H}_{505}\text{O}_{21}$  formula, at natural abundance (Figure 7B). Now the “excess” of the experimental intensity on the low  $m/z$  side of the  $(M - \text{OCH}_3)^+$  ion appears to be increased, compared to that in **2-(OMe)<sub>15</sub>**. All other peaks in the  $m/z$  2000–8000 range have relatively small amplitude (<3%). The doubly charged  $(M - 2\text{OCH}_3)^{2+}$  ion possesses an isotopic cluster near  $m/z$  3043; the experimental and calculated isotopic intensities are in a good agreement. The peak corresponding to the loss of the outer “module with benzene ring” appears at  $m/z$  4137 (less  $m/z$  1980) in the low-resolution spectrum.

For 36-ether **4-(OMe)<sub>36</sub>**, the low-resolution FABMS shows the two most intense peaks at  $m/z$  10022 (100%) and 4995 (85%) (Figure 8A). Both peaks have similar fragmentation patterns;

however, the  $m/z$  spacings between the fragmentation ions for the  $m/z$  4995 region ( $m/z$  7–8) are approximately half of those for the  $m/z$  10022 region. Also, the widths of the isotopic envelopes appear narrower for the  $m/z$  4995 region compared to the  $m/z$  10022 region. This suggests that the peaks at  $m/z$  10022 and 4995 correspond to singly and doubly charged ions  $(M - \text{OCH}_3)^+$  and  $(M - 2\text{OCH}_3)^{2+}$ , respectively. The positions of the remaining peaks at  $m/z$  7761, 3865, and 4479 are matched well by the low-resolution spectrum of a mixture, containing the side products such as **19-(OMe)<sub>28</sub>** and **20A-(OMe)<sub>15</sub>(OH)** (Figure 8B).<sup>43,44</sup> The minor peaks at  $m/z$  7761 and 3865 are assigned to the side product **19-(OMe)<sub>28</sub>**; these two peaks correspond to the singly and doubly charged ions  $(M - \text{OCH}_3)^+$  and  $(M - 2\text{OCH}_3)^{2+}$ , respectively. The small peak at  $m/z$  4479 may be the  $(M - \text{OCH}_3)^+$  ion for the “demethylation product” side product **20A-(OMe)<sub>15</sub>(OH)**. Because the ionization efficiency for polyarylmethyl polyethers decreases dramatically in relation to mass, the relative intensities of the ions observed in the mass spectra are severely distorted, overestimating relative content of the side products with lower molecular weights.<sup>30a,43,44</sup>

For the  $(M - \text{OCH}_3)^+$  ion of **4-(OMe)<sub>36</sub>**, the high-resolution spectra for two different samples give the peak maxima at  $m/z$  10021.5 and 10021.9; these values are 1–2 amu below the calculated average mass (10023.45) and peak maximum mass (10023.04) for the formula  $\text{C}_{719}\text{H}_{821}\text{O}_{35}$  for the  $(M - \text{OCH}_3)^+$  ion cluster. Considering the instrumental limitations and the observed shifts to the lower  $m/z$  for the isotopic clusters from homologous polyethers, this 1–2 amu mass difference may not be unusual in this high  $m/z$  range. Also, the isotopic envelope for the  $(M - \text{OCH}_3)^+$  ion of **19-(OMe)<sub>28</sub>** is somewhat shifted to the lower  $m/z$  values, compared to the simulated envelope for the formula  $\text{C}_{557}\text{H}_{635}\text{O}_{27}$  at the natural isotopic abundance (Figure 8B).

**2.1.3.B. Gel Permeation Chromatography with Multiangle Light Scattering (GPC/MALS) and Small Angle Neutron Scattering (SANS) of Target Polyethers.** Polyethers **2-(OMe)<sub>15</sub>**, **3-(OMe)<sub>22</sub>**, and **4-(OMe)<sub>36</sub>** elute in the expected order of increased hydrodynamic radii for greater molecular weights (Figure 3s, Supporting Information). The weight-average molecular masses ( $M_w$ ) for **2-(OMe)<sub>15</sub>**, **3-(OMe)<sub>22</sub>**, and **4-(OMe)<sub>36</sub>** are  $\sim 5$ ,  $\sim 7.5$ , and  $\sim 12$  kDa, respectively; the polydispersities ( $\text{PD} = M_w/M_n$ ) are in the 1.00–1.02 range, as expected for monodisperse oligomers (Table 6s, Supporting Information). Assuming that only about  $\sim 80\%$  of the injected mass of polyether is eluted, good agreement with the formula masses is obtained. Similar discrepancies between the  $M_w$  and the formula mass were also observed for other polyarylmethyl polyethers.<sup>1,30a,45</sup>

Radii of gyration ( $R_g$ ) for polyethers **2-(OMe)<sub>15</sub>**, **3-(OMe)<sub>22</sub>**, and **4-(OMe)<sub>36</sub>** in tetrahydrofuran- $d_8$  (THF- $d_8$ ) are 1.2, 1.3, and 1.8 nm, respectively, as determined by small angle neutron scattering (SANS).<sup>46</sup>

(43) GPC/MALS for the identical sample of **19-(OMe)<sub>28</sub>**, which was used for the FABMS in Figure 8B, shows two peaks with the relative peak amplitudes of about 10:1. For the more intense peak, which is found at the shorter elution time, the corrected  $M_w$  (assuming  $\sim 80\%$  elution fraction) approximately matches the formula mass for **19-(OMe)<sub>28</sub>**. The minor peak observed in GPC/MALS is tentatively assigned to **20A-(OMe)<sub>15</sub>(OH)**.

(44) The  $^1\text{H}$  NMR spectra for the sample of **4-(OMe)<sub>36</sub>**, for which FABMS is shown in Figure 8A, indicate that relative integration for **19-(OMe)<sub>28</sub>** is about 10%.

(45) For **4-(OMe)<sub>36</sub>**, contribution from about 10% content of **19-(OMe)<sub>28</sub>** (ref 44) to the measured  $M_w$  would be negligible, considering other sources of error.

**2.1.3.C. NMR Spectroscopy of Target Polyethers.**  $^1\text{H}$  NMR (500 MHz) spectra for polyethers **2-(OMe)<sub>15</sub>**, **3-(OMe)<sub>22</sub>**, and **4-(OMe)<sub>36</sub>** are recorded in benzene-*d*<sub>6</sub> at 293, 328, and 348 K. The best resolved spectra are typically obtained at the highest available temperature (348 K).

For pentadecaether **2-(OMe)<sub>15</sub>**,  $^1\text{H}$  NMR spectra are slightly different for the two isolated fractions and each fraction shows a mixture of at least two diastereomers. Only the fraction of higher  $R_f$ , which is used for further studies (including generation of polyradicals), is analyzed. Both the *tert*-butyl group and the methoxy group regions contain 10–13 resonances; few of them are broadened and only partially resolved at 293 and 348 K. When integrations of the *tert*-butyl group region and the methoxy group region are normalized to a single diastereomer, few resonances with fractional integrations (e.g., 3 H in the *tert*-butyl group region) are found, as expected for a mixture of diastereomers.

For a 2-fold-symmetric stereoisomer of **2-(OMe)<sub>15</sub>**, four 1,3,5-trisubstituted and 12 1,4-disubstituted benzene rings are expected in the aromatic region of  $^1\text{H}$  NMR spectrum.  $^1\text{H}$ – $^1\text{H}$  COSY spectra at and 293 and 348 K may be assigned for 1,3,5-trisubstituted benzene rings; all 24 cross-peaks for the expected four sets of three 2-proton  $J = 2$  triplets are found (Figure 4s, Supporting Information). However, selected 2-proton “triplets” are broadened or split into two nearly overlapping triplets, and their cross-peaks are distorted from the usual shape. The spectrally congested 1,4-disubstituted benzene rings are not assigned.

For 22-ether **3-(OMe)<sub>22</sub>**,  $^1\text{H}$  NMR spectra at 293, 328, or 348 K show a mixture of at least two diastereomers (Figures 5s–8s, Supporting Information). The *tert*-butyl group region is too congested for a meaningful analysis. Only about half of the expected 30 resonances (for one diastereomer) are resolved in the 1.27–1.13 ppm region.

In the methoxy group region of the  $^1\text{H}$  NMR spectra, 22 distinct 3-proton singlets are expected for each diastereomer. At 348 K, 21 distinct resonances are resolved; however, five singlets integrate only to about 0.9–1.0 protons each and two other singlets (with similar chemical shifts) integrate together to 1.6 protons. An analogous spectrum, with 26 distinct resonances, is obtained at 293 K; in particular, the most downfield 3-proton singlet at 348 K (at 3.106 ppm) splits into two singlets (3.104 and 3.100 ppm) (Figure 6s, Supporting Information).

In the aromatic region of the  $^1\text{H}$  NMR spectrum (and  $^1\text{H}$ – $^1\text{H}$  COSY) for **3-(OMe)<sub>22</sub>**, 12 1,3,5-trisubstituted and 34 1,4-disubstituted benzene rings are expected for each diastereomer. The best resolved  $^1\text{H}$ – $^1\text{H}$  COSY spectrum at 348 K could only be assigned in part for 1,3,5-trisubstituted benzene rings; the cross-peaks for 1,4-disubstituted benzene rings are very congested (Figure 8s, Supporting Information). Twelve sets of three 1-proton  $J = 2$  triplets are expected for 12 1,3,5-trisubstituted benzene rings. In the actual spectrum, many resonances are broadened, resulting in the absence of several cross-peaks. Three sets of three 1-proton resonances and four sets of three 2-proton resonances are found; one set of three 1-proton resonances could not be identified. Most of the 1- and 2-proton resonances with the resolved coupling appear as pairs of nearly coincident  $J = 2$  triplets ( $\Delta\delta \approx 0.003$ – $0.004$  ppm); this additional splitting of

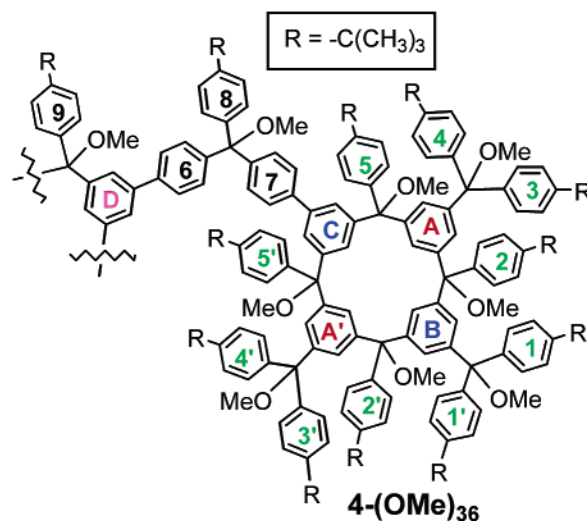


**Figure 9.** 36-Ether **3-(OMe)<sub>36</sub>** with numbering scheme for the assignment of NMR spectra.

the 1-proton resonances is consistent with the presence of diastereomers.

$^1\text{H}$  NMR spectra of 36-ether **4-(OMe)<sub>36</sub>** at 348 K show one predominant isomer, in which the outer and the inner calix[4]-arene rings are approximately 2-fold and tetra-fold symmetric, respectively (Figure 9).

In the *tert*-butyl group region, six singlets (36, 72, 72, 72, 72, 72 protons) in the 1.18–1.26 ppm range and an upfield-shifted 36-proton set of five singlets in the 1.07–1.09 ppm range (resembling a pentuplet) are found (Figure 10). Because this upfield group of resonances becomes increasingly complex at lower temperatures (328 and 293 K), conformational equilibria or diastereomers may be involved. The possibility of a conformation with lower than tetrafold symmetry (on the NMR time scale) or the presence of more than one diastereomer may be illustrated by the splitting of the 36-proton singlet at 348 K into a pair of 18-proton singlets ( $\Delta\delta \approx 0.003$  ppm) at 293 K (Figure 10).

Six singlets (1:1:1:1:2:3) are found in the methoxy group region of the  $^1\text{H}$  NMR (500 MHz, 348 K) spectrum (Figure 9s, Supporting Information), suggesting that at least one pair of the methoxy groups is diastereotopic, analogously to that found in module-with-linker **15A**. Except for the most downfield 12-proton broad singlet at 3.176 ppm, the remaining singlets are within the 3.01–2.89 ppm range, which is similar to that for **11A** and **15A**.

The aromatic region of the  $^1\text{H}$  NMR spectrum (and  $^1\text{H}$ – $^1\text{H}$  COSY) for **4-(OMe)<sub>36</sub>** at 348 K shows 10 and eight cross-peaks between the  $J = 2$  and  $J = 8$ – $9$  multiplets, respectively (Figure 11). The  $J = 2$  multiplets appear as three correlated sets: the first set has one pair of nearly coincident ( $\Delta\delta \approx 0.004$  ppm) 4-proton triplets and two 8-proton triplets (rings A and A', Figures 9 and 11), and each of the other two sets consists of a 4-proton triplet and 8-proton doublet (rings B and C, Figures 9 and 11). Two broad singlets at 8.015 (4 H) and 7.936 (8 H) ppm, which do not show a COSY cross-peak, account for the four 1,3,5-trisubstituted benzene rings of the macrocyclic core (ring D, Figures 9 and 11). The remaining resonances in the aromatic region account for all 1,4-disubstituted benzene rings (rings 1–9, Figures 9 and 11): 10 16-proton and six 8-proton doublets ( $J = 8$ – $9$ ) are correlated pairwise in the  $^1\text{H}$ – $^1\text{H}$  COSY

(46) The values of  $R_g$  are obtained from the Guinier fits in the  $q$ -ranges, for which  $R_g q < 1.10$ . The small angle neutron scattering (SANS) experiments and the data handling are described in Supporting Information.

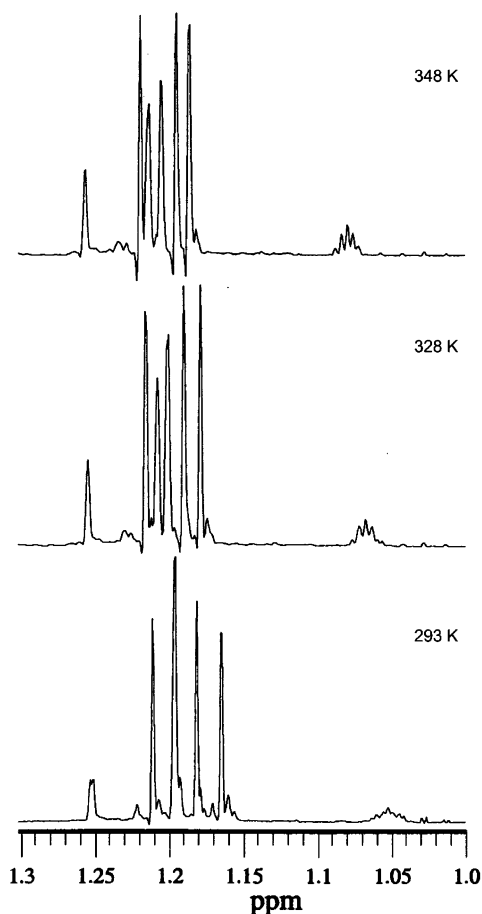


**Figure 10.**  $^1\text{H}$  NMR (500 MHz, benzene- $d_6$ ) spectra for the *tert*-butyl group region of **4-(OMe)<sub>36</sub>**.

spectrum, and two 8-proton singlets at 7.443 and 7.438 ppm are interpreted as a nearly isochronous AB system. In the one bond  $^{13}\text{C}$ – $^1\text{H}$  coupling HMQC experiment at 348 K (Figure 10s, Supporting Information),  $^1\text{H}$  resonances in the aromatic region show the expected cross-peaks (with a few spectral overlaps), except for the four broadened peaks at 8.015 (bs), 7.936 (bs), 7.661 (bt,  $J \approx 2$  Hz), and 7.594 (bd,  $J \approx 9$  Hz) ppm.

Overall, NMR spectra for **4-(OMe)<sub>36</sub>** at 348 K may be viewed as superposition of the spectra for the macrocyclic core **18** and four module-with-linkers **15A**, less differences in chemical shifts and dynamic behavior.

Direct comparison of the  $^1\text{H}$  NMR spectra for **4-(OMe)<sub>36</sub>** and **20A-(OMe)<sub>16</sub>** provides additional evidence for the spectral assignments for **4-(OMe)<sub>36</sub>** (Figures 12–14). For a homocoupling product of racemic module-with-linker **15A**, two diastereomers are expected, i.e., the pair of enantiomers and the meso compound. The  $^1\text{H}$  NMR spectra for **20A-(OMe)<sub>16</sub>** show the expected 2-fold symmetry at 293, 328, and 348 K. However, the 18-proton resonance in the *tert*-butyl group region is split into two overlapping singlets of equal peak height (the most downfield peaks at 1.237 and 1.236 ppm at 348 K) (Figure 13). Analogous splitting of the most downfield 36-proton resonance in the *tert*-butyl group region is observed for **4-(OMe)<sub>36</sub>** at 293 K. The spectral differences between the two compounds allow for identification of the resonances for the macrocyclic core of **4-(OMe)<sub>36</sub>** at 348 K (ring 9 with the *tert*-butyl group, methoxy group, and ring D, Figure 9): (1) in the *tert*-butyl group region, the upfield-shifted 36-proton set of five

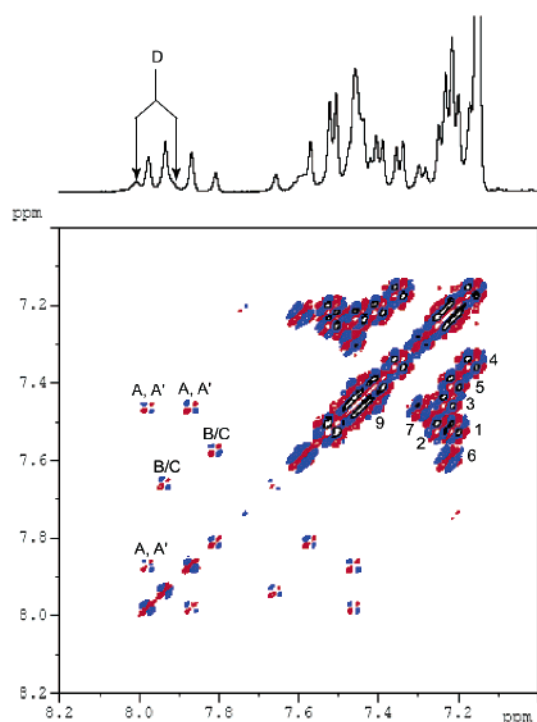


**Figure 11.**  $^1\text{H}$ – $^1\text{H}$  DQF COSY NMR (500 MHz, benzene- $d_6$ ) spectrum for **4-(OMe)<sub>36</sub>** at 348 K.

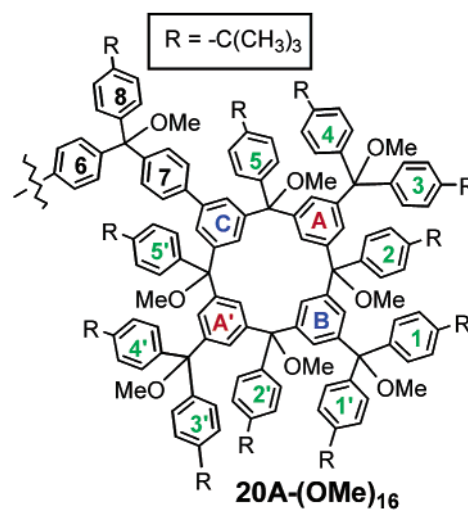


**Figure 12.** Polyether **20A-(OMe)<sub>16</sub>** with numbering scheme for the assignment of  $^1\text{H}$  NMR spectra.

singlets in the 1.07–1.09 ppm range (Figure 13), (2) in the methoxy group region, the most downfield, broad 12-proton singlet at 3.176 ppm (Figure 13), and (3) in the aromatic region, two broad singlets at 8.015 (4 H), 7.936 (8 H) ppm and two COSY-correlated doublets at 7.457 ( $J = 8$ , 8 H), 7.410 ( $J = 8$ , 8 H) (Figure 14). This accounts for all  $^1\text{H}$  resonances of the macrocyclic core. The degree of broadening and chemical shifts may suggest that two 8-proton COSY-correlated doublets at 7.594 (broad) and 7.223 ppm (at 348 K) correspond to the 1,4-connected benzene ring (ring 6, Figure 9) adjacent to the macrocyclic core (Figure 14).

**2.2. Generation of Polyradicals 2, 3, and 4.** Polyethers **2-(OMe)<sub>15</sub>**, **3-(OMe)<sub>22</sub>**, and **4-(OMe)<sub>36</sub>** (0.8–2.1 mg per sample) are converted to the corresponding polyradicals **2**, **3**, and **4**, respectively. The relevant chemistry and technical procedures



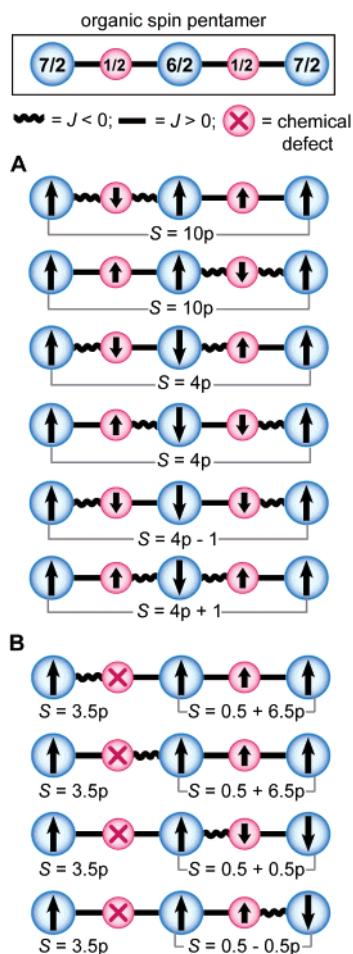


**Figure 15.** Organic spin pentamer of component spins,  $7/2$ ,  $1/2$ ,  $6/2$ ,  $1/2$ ,  $7/2$ , corresponding to 22-radical **3**. (A) Spin systems for the configuration with two antiferromagnetic ( $J < 0$ ) couplings through the biphenylene coupling units and zero chemical defects at the 4-biphenyl-substituted sites. (B) Spin systems for the configuration with one antiferromagnetic ( $J < 0$ ) coupling through the biphenylene coupling units and one chemical defect at the 4-biphenyl-substituted sites.

component spins,  $7/2$ ,  $1/2$ ,  $6/2$ ,  $1/2$ ,  $7/2$ , are connected via four biphenylene coupling units.

Overall, 15 configurations, with 0–4 antiferromagnetic ( $J < 0$ ) couplings through biphenylene coupling units and 0–2 chemical defects at the 4-biphenyl-substituted sites, are considered. Two representative configurations are analyzed.

The first configuration involves two antiferromagnetic ( $J < 0$ ) couplings through biphenylene coupling units and zero chemical defects at the 4-biphenyl-substituted sites (Figure 15A). For this configuration, there are six ways to distribute two antiferromagnetic ( $J < 0$ ) and two ferromagnetic ( $J > 0$ ) biphenylene coupling units, leading to the following spin systems:  $S = 10p$ ,  $S = 10p$ ,  $S = 4p$ ,  $S = 4p$ ,  $S = 4p - 1$ , and  $S = 4p + 1$ .

The second configuration involves one antiferromagnetic ( $J < 0$ ) coupling through biphenylene coupling units and one chemical defect at the 4-biphenyl-substituted sites (Figure 15B). In the presence of one chemical defect at the 4-biphenyl-substituted site, there are four ways to distribute one antiferromagnetic ( $J < 0$ ) and three ferromagnetic ( $J > 0$ ) biphenylene coupling units, leading to the following eight spin systems:  $S = 3.5p$ ,  $S = 3.5p$ ,  $S = 3.5p$ ,  $S = 3.5p$ ,  $S = 0.5 + 6.5p$ ,  $S = 0.5 + 6.5p$ ,  $S = 0.5 + 0.5p$ ,  $S = 0.5 - 0.5p$ . Because there are two

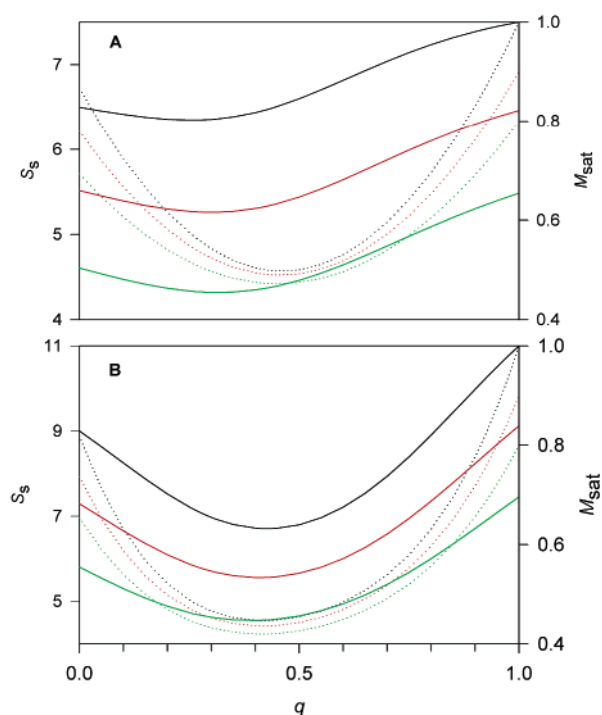


**Figure 16.** Plots of average spin ( $S_s$ , full lines) and magnetization at saturation ( $M_{\text{sat}}$ , dotted lines) for percolation model (eq 2) for pentadecaradical **2** (plot A) and 22-radical **3** (plot B). The black, red, and green lines correspond to parameter  $p$  set to 1.0, 0.9, and 0.8, respectively.

ways to distribute one chemical defect between the two 4-biphenyl-substituted sites, the actual number of spin systems is doubled from eight to 16.

Overall, 128 spin systems are enumerated from 15 configurations for the organic spin pentamer, corresponding to 22-radical **3**. Each spin system, derived from the configuration with  $r$  ferromagnetic ( $J > 0$ ) biphenylene coupling units and  $s$  unpaired electrons, enters into the linear combination of Brillouin functions (eq 2) with a factor of  $b_{r,s} = [q^r(1 - q)^{4-r}][p^s(1 - p)^{2-s}]$ . (Detailed equations are provided in the Supporting Information: eqs 1s–7s and Table 7s.)

Analogous procedure for enumeration of spin systems with respect to parameters  $q$  and  $p$  is applied to the organic spin trimer, corresponding to pentadecaradical **2**. Overall, six configurations, with 0–2 antiferromagnetic ( $J < 0$ ) couplings through biphenylene coupling units and 0–1 chemical defects at the 4-biphenyl-substituted sites are considered. Each spin system, derived from the configuration with  $r$  ferromagnetic ( $J > 0$ ) biphenylene coupling units and  $s$  unpaired electrons, enters into the linear combination of Brillouin functions (eq 2) with a factor of  $b_{r,s} = [q^r(1 - q)^{2-r}][p^s(1 - p)^{1-s}]$ .

Values for  $S_s$ ,  $M_{\text{sat}}$ , and  $\chi T_{\text{max}}$  are calculated from the variable parameters  $q$  and  $p$ . The behavior of  $S_s$  and  $M_{\text{sat}}$  within this percolation model (eq 2) is shown in Figure 16.

For pentadecaradical **2** with  $p = 1.0$  (no chemical defects),  $S_s$  as a function of  $q$  has a shallow minimum  $S_s \approx 6.35$  at  $q \approx 0.25$ ; as expected, the limiting values are  $S_s = 6.5$  for  $q = 0$  (all-antiferromagnetic couplings) and  $S_s = 7.5$  for  $q = 1.0$  (all-ferromagnetic couplings). For  $M_{\text{sat}}$ , the minimum value  $M_{\text{sat}}(\text{min}) \approx 0.50$  is found at  $q(\text{min}) \approx 0.4$ ; at this value of  $q$ ,  $S_s$  is approximately equal to 6.4 ( $S_s \approx 6.4$ ). For 22-radical **3** with  $p = 1.0$ , relatively deep minima  $S_s \approx 6.71$  and  $M_{\text{sat}} \approx 0.447$  both at  $q \approx 0.4$  are found; the limiting values are  $S_s = 9$  for  $q = 0$

**Table 1.** Summary of Magnetic Data and Numerical Fits to the Percolation Model and Eq 1 ( $S_2 = 1/2$ ) for Pentadecaradical **2** at  $T = 1.8$  K<sup>a</sup>

sample label	mass <sup>a</sup>		parameter dependence		$S_s$	$M_{\text{sat}}^b$ ( $\mu_B$ )		$\chi T_{\text{max}}^c$ ( $\text{emuKmol}^{-1}$ )		$S_s^d$
	(mg)	$q$	$p$	eq 2		eq 2	eq 2	eq 2	eq 2	
1552	0.98	0.88	0.79	0.961	5.2	0.67	0.67	15.7	15.4	5.1
1561	1.30	0.80	0.86	0.932	5.7	0.64 <sup>e</sup>	0.64	16.2 <sup>e</sup>	16.0	5.6 <sup>e</sup>
1590	1.00	0.75	0.79	0.940	4.9	0.57	0.57	12.6	12.5	4.8
1652	0.91	0.74	0.89	0.896	5.8	0.60	0.60	15.2	15.2	5.7

<sup>a</sup> Mass of pentadecaether **2**-(OMe)<sub>15</sub>. <sup>b</sup>  $M_{\text{sat}}$  per mole of triarylmethyl ether. <sup>c</sup>  $\chi T_{\text{max}}$  per mole of **2**-(OMe)<sub>15</sub> measured at 500 Oe. <sup>d</sup> Numerical fit using eq 1 with three variable parameters and parameter dependence within the 0.64–0.90 range for all samples. <sup>e</sup> After annealing at 293 K for about 30 min,  $M_{\text{sat}} = 0.41 \mu_B$ ,  $\chi T_{\text{max}} \approx 8 \text{ emuKmol}^{-1}$ , and  $S_s \approx 3.7$  (eq 1 with three variable parameters).

and  $S_s = 11$  for  $q = 1.0$ . For both **2** and **3**, when  $p = 0.9$  and  $p = 0.8$ , the  $S_s$  is significantly shifted to lower values.  $M_{\text{sat}}$  has relatively small dependence with respect to  $p$ . This suggests that in the presence of random antiferromagnetic couplings, relatively large values of  $S_s$  are still possible, even with relatively small fraction of unpaired electrons remaining at low temperature.

**2.4. Magnetic Studies of Polyradicals 2, 3, and 4.** For a typical sample of polyradical in THF-*d*<sub>8</sub>, magnetization ( $M$ ) is measured as a function of magnetic field ( $H = 0$ – $5 \times 10^4$  Oe at five or four temperatures in the  $T = 1.8$ – $10$  K range) and temperature ( $T = 1.8$ – $150$  K at  $H = 5000$  Oe and, for selected samples, 500 and/or 50 Oe). For selected samples, the following sequences of measurements are carried out: first, without annealing (with sample chamber degassed at 90 K); second, with prior annealing at 170 K (slightly above the melting point of the matrix); and third, after exposure of the sample to room temperature for a short period (30–70 min). After completion of these measurements, point-by-point background corrections for diamagnetism are carried out (Experimental Section).

The results and discussion of magnetic studies are summarized and illustrated in Tables 1–3 and Figures 17–19.

**2.4.1. Magnetic Data for Polyradicals 2, 3, and 4, Which Are Strictly Handled at Low Temperatures ( $T \leq 170$  K).** Numerical fits to the  $M$  vs  $H/T$  data for **2**, using the percolation model (eq 2), give  $q = 0.74$ – $0.88$  and  $p = 0.79$ – $0.89$  (Table 1). The optimized values of  $q$  and  $p$  correspond to spin-average spin,  $S_s = 4.9$ – $5.8$ . Similar values of  $S_s$  are obtained from the numerical fits of the  $M$  vs  $H/T$  data, using eq 1 (Table 1, last column).<sup>48</sup> As expected for  $q, p < 1$ ,  $S_s$  is less than  $15/2$ , the theoretical value of  $S$  for defect-free, ferromagnetically coupled pentadecaradical. Most interestingly, the values of  $M_{\text{sat}} = 0.57$ – $0.67 \mu_B$  are in quantitative agreement with the experiment (Table 1). The quality of the numerical fits is illustrated in Figure 17 for a sample of **2** with  $S_s \approx 5.8$ .

Excellent numerical fits to the  $M$  vs  $H/T$  data for **3** are obtained as illustrated in Figure 18. A relatively narrow range of  $q = 0.75$ – $0.81$  and large values of  $p = 0.90$ – $1.00$  are obtained, compared to **2** (Table 2). The three samples of **3** with the largest values of parameter  $p = 0.98$ – $1.00$  have the largest values of  $S_s = 8$ – $9$ , near the theoretical value of  $S = 11$  for defect-free, ferromagnetically coupled 22-radical.<sup>49</sup> Parameter

(48) For numerical fits of the  $M$  vs  $H/T$  data for pentadecaradical **2** at 1.8 K, using eq 1, moderate parameter dependence in the 0.67–0.89 range is found.

(49) This near perfect generation of 22-radical **3** may be the result of a more extensive effort in its generation; only a subset of samples is reported.

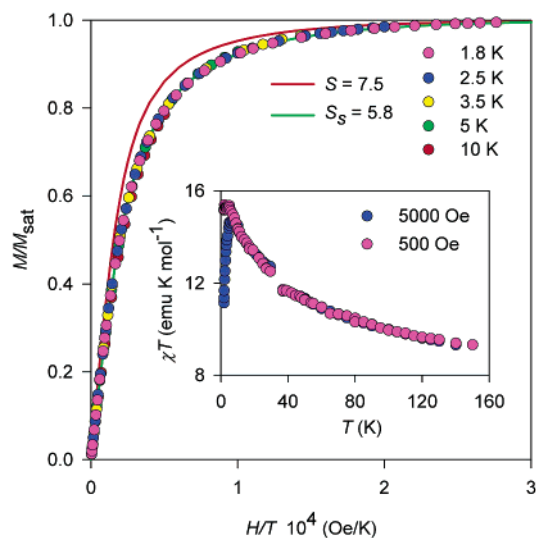


**Figure 17.** SQUID magnetometry for pentadecaradical **2** in THF-*d*<sub>8</sub> (sample label 1652, Table 1). Main plot:  $M/M_{\text{sat}}$  vs  $H/T$ . Solid lines, labeled  $S = 7.5$  and  $S_s = 5.8$ , correspond to plots of Brillouin function with  $S = 7.5$  and numerical fit of the experimental data at 1.8 K using the percolation model, respectively. Inset plot:  $\chi T$  vs  $T$ .

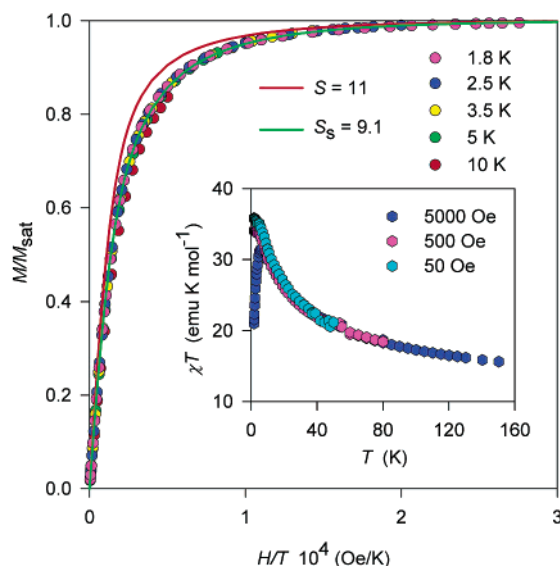


**Figure 18.** SQUID magnetometry for 22-radical **3** in THF-*d*<sub>8</sub> (sample label 1594, Table 2). Main plot:  $M/M_{\text{sat}}$  vs  $H/T$ . Solid lines, labeled  $S = 11$  and  $S_s = 9.1$ , correspond to plots of Brillouin function with  $S = 11$  and numerical fit of the experimental data at 1.8 K using the percolation model, respectively. Inset plot:  $\chi T$  vs  $T$ .

dependence is in the 0.92–0.95 range. Similar values of  $S_s$  could be obtained from fits to eq 1; however, the use of four variable parameters, which are necessary to reproduce the curvature of magnetization for **3**, leads to overparametrization. The values of  $M_{\text{sat}} = 0.57$ – $0.65 \mu_B$  are nearly identical to those in **2**. The agreement between the percolation model and the experiment is excellent for values of  $M_{\text{sat}}$  (Table 2).<sup>50</sup>

The percolation model (eq 2) is not developed for hexa-tricontaradical (36-radical) **4**. Explicit enumeration of very

(50) As mentioned earlier in the text and discussed in a greater detail in ref 1, an incomplete mass transfer may lead to an underestimate of values of  $M_{\text{sat}}$  (and  $\chi T$ ), which are calculated on the basis of the weighed masses of polyethers. For **2** and **3**, numerical fits to the percolation model, which include the mass of the polyether as a third variable parameter, are overparametrized; the fitted masses are typically greater (by 10–20%), compared to the weighed masses.

**Table 2.** Summary of Magnetic Data and Numerical Fits to the Percolation Model ( $T = 1.8$  K) for 22-Radical **3**<sup>a</sup>

sample label	mass <sup>a</sup> (mg)	$q$	$\rho$	parameter dependence	$S_s$	$M_{\text{sat}}^b$ ( $\mu_B$ )		$\chi T_{\text{max}}^c$ (emuKmol <sup>-1</sup> )	
				eq 2		eq 2	eq 2	eq 2	
1010	2.09	0.79	0.91	0.947	7.4	0.59	0.59	24.9	27.2
1168	1.21	0.77	0.99	0.924	8.5	0.60	0.60	30.3	31.2
1231 <sup>d</sup>	1.50	0.77	0.95	0.938	7.9	0.59	0.59	27.9	28.6
1327	0.97	0.78	0.90	0.949	7.1	0.57	0.57	25.5	25.5
1594 <sup>e</sup>	0.89	0.81	1.00	0.932	9.1	0.65	0.65	35.9	35.9
1636	0.89	0.75	0.98	0.919	8.2	0.58	0.58	28.9	29.1

<sup>a</sup> Mass of 22-ether **3**-(OMe)<sub>22</sub> (sample labels 0997 and 1555). <sup>b</sup>  $M_{\text{sat}}$  per mole of triarylmethyl ether. <sup>c</sup>  $\chi T_{\text{max}}$  per mole of **3**-(OMe)<sub>22</sub> measured at 500 Oe. <sup>d</sup> Numerical fit at 3 K and  $\chi T_{\text{max}}$  at 200 Oe. <sup>e</sup> After annealing at 293 K for about 50 min,  $S_s \approx 3.7$  (eq 1),  $M_{\text{sat}} = 0.33 \mu_B$ , and  $\chi T_{\text{max}} = 9.2$  emuKmol<sup>-1</sup>.

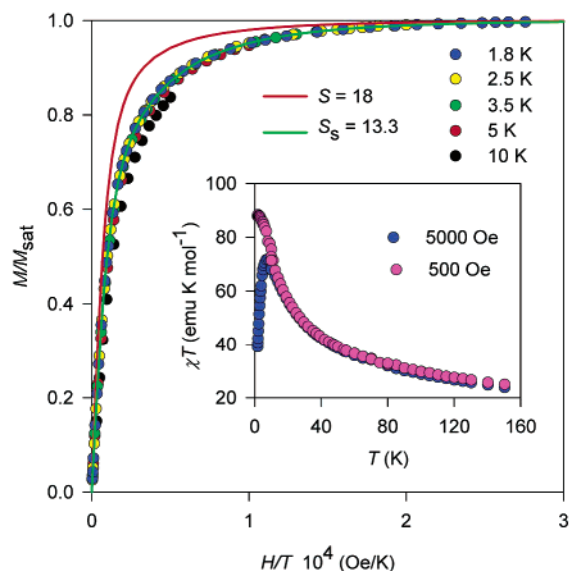


**Figure 19.** SQUID magnetometry for 36-radical **4** in THF-*d*<sub>8</sub> (sample label 1620, Table 3). Main plot:  $M/M_{\text{sat}}$  vs  $H/T$ . Solid lines, labeled  $S = 18$  and  $S_s = 13.3$ , correspond to plots of Brillouin function with  $S = 18$  and numerical fit of the experimental data at 1.8 K, respectively. The numerical fit is based upon linear combination of two Brillouin functions (eq 1) with four variable parameters. Inset plot:  $\chi T$  vs  $T$ .

large number of possible  $r,s$ -configurations would not be practical. Furthermore, side products found in 36-ether **4**-(OMe)<sub>36</sub> would further complicate the percolation model. Numerical fits using eq 1 with four variable parameters give values of  $S_s = 8$ –13 for 36-radical **4**; for the four best samples of **4**,  $S_s = 12$ –13, still significantly below  $S = 18$  for defect-free, ferromagnetically coupled 36-radical. The values of  $M_{\text{sat}}$  are in the  $0.41$ – $0.72 \mu_B$  range; however,  $M_{\text{sat}}$  is in the  $0.63$ – $0.72 \mu_B$  range for the best four samples (Figure 19, Table 3). There is no obvious correlation between the experimental values of  $S_s$  and  $M_{\text{sat}}$ .

The  $M$  vs  $T$  data at  $H = 5000$ , 500, and/or 50 Oe are plotted as the product of magnetic susceptibility per mole of starting polyether ( $\chi = M/H$ ) and temperature vs temperature, i.e.,  $\chi T$  vs  $T$  for polyradicals **2**, **3**, and **4** (inset plots in Figures 17–19). For all polyradicals, the values of  $\chi T$  are increasing with decreasing temperature from 150 to about 5 K, indicating the thermal depopulation of the low spin excited states. This behavior is consistent with the presence of a weak ferromagnetic coupling. In the  $T = 5$ –1.8 K range and low magnetic fields (e.g., 500 or 50 Oe), a nearly flat curve (plateau) and a slower

**Table 3.** Summary of Magnetic Data and Numerical Fits to the Linear Combination of Brillouin Functions (Eq 1, Four Variable Parameters,  $T = 1.8$  K) for 36-Radical **4**<sup>a</sup>

sample label	polyether synth no. <sup>a</sup>	mass <sup>b</sup> (mg)	anneal (K)	$S_s$	$M_{\text{sat}}^c$ ( $\mu_B$ )	parameter dependence	$\chi T_{\text{max}}^d$ (emuKmol <sup>-1</sup> )
						eq 2	
1111	I	1.65	170	12	0.62	0.45–0.99	58 (5000)
1339	I	0.78	170	8	0.41	0.57–0.98	29 (5000)
1595	II	0.91	170	11	0.63	0.55–0.99	71 (50)
				7	0.45	0.59–0.99	34 (50)
1620	III	0.84	170	13	0.70	0.62–0.97	88 (500)
				293 <sup>e</sup>	dia	dia	dia
1670	III	1.11	$\leq 170$	12	0.56	0.61–0.98	70 (50)
				293 <sup>e</sup>	dia	dia	dia
1686	III	1.10	$\leq 170$	12.5	0.72	0.64–0.98	86 (500)
				293 <sup>f</sup>	5	0.38	0.68–0.99

<sup>a</sup> 36-ether **4**-(OMe)<sub>36</sub> from three different syntheses was used (Experimental Section). <sup>b</sup> Mass of 36-ether **4**-(OMe)<sub>36</sub>. <sup>c</sup>  $M_{\text{sat}}$  per mole of triarylmethyl ether. <sup>d</sup>  $\chi T_{\text{max}}$  per mole of **4**-(OMe)<sub>36</sub> measured at indicated magnetic field (Oe). <sup>e</sup> Annealing for about 30 min. <sup>f</sup> Annealing for about 70 min.

rise in  $\chi T$  with decreasing temperature down to 1.8 K are obtained for **2** and its higher homologues, respectively.<sup>51</sup>

The approximate ideal paramagnetic behavior for **2** at low temperatures found in the  $\chi T$  vs  $T$  plots is consistent with the use of the Brillouin functions for the  $M$  vs  $H$  data. Because the net ferromagnetic couplings in **3** and **4** span the whole temperature range down to 1.8 K, the numerical fits to the Brillouin functions (eqs 1 and 2) may not be adequate. However, such numerical fits still provide useful approximation, i.e., excellent agreement between the experiment and the percolation models is obtained in **2** and **3** for the maximum values of  $\chi T$  at low temperature ( $\chi T_{\text{max}}$ ). Also, this agreement illustrates accuracy of the percolation models at both high  $H$  ( $M_{\text{sat}}$ ) and low  $H$  ( $\chi T_{\text{max}}$ ) regimes.

The maximum values of  $\chi T$  for the plateau at low temperature ( $\chi T_{\text{max}}$ ) are below those for the defect-free ferromagnetically coupled polyradicals (Figures 17–19); this is consistent with the less than expected values of  $S$  and  $M_{\text{sat}}$ . For the four best samples of **2**, **3**, and **4**,  $\chi T_{\text{max}}$  values are 13–16, 28–36, and 70–88 emuKmol<sup>-1</sup>, respectively; the monodisperse  $S = 15/2$ ,  $S = 11$ , and  $S = 18$  polyradicals should give  $S(S + 1)/2 = 31.875$ , 66, and 171 emuKmol<sup>-1</sup>, respectively.

#### 2.4.2. Thermal Stability (Persistence) of Polyradicals.

Selected samples of polyradicals are studied after exposure to room temperature for about 0.5–1 h. In each case, only eq 1 is employed for numerical fits to the  $M$  vs  $H/T$  data; the percolation models do not give adequate fits, as expected. For a sample of **2** ( $S_s = 5.7$ ,  $M_{\text{sat}} = 0.64 \mu_B$ , and  $\chi T_{\text{max}} \approx 16$  emuKmol<sup>-1</sup>), the corresponding values are 3.7,  $0.41 \mu_B$ , and 8 emuKmol<sup>-1</sup>, after annealing at room temperature for about 30 min (Table 1). Similar behavior is found for one sample of **3** after annealing at room temperature for about 50 min, i.e., the value of  $S_s$  decreases from 9.1 to 3.8 and the value of  $M_{\text{sat}}$  decreases by about factor of 2 (Table 2). Four samples of **4** are annealed at room temperature for 30–70 min (Table 3). For two of the samples with  $S_s = 11$  and  $S_s = 12.5$ , after 30 and 70 min at room temperature,  $S_s = 7$  and  $S_s = 5$  are obtained, respectively. However, the other two samples of **4** become diamagnetic after 30 min at room temperature. One possibility is that excess of iodine is present in those samples and it reacts with radicals at higher temperature. Overall, polyradicals **2**–**4** are relatively

(51) The downward turn in  $\chi T$  at  $H = 5000$  Oe is caused by the paramagnetic saturation, as illustrated in Figure 11s, Supporting Information.

persistent at room temperature;  $S_s = 7$  for **4** is the highest value of  $S$  in a polyradical exposed to room temperature for an extended period.

### 3. Conclusion

Polyarylmethyl polyethers, in which calix[4]arene-based macrocyclic modules are connected with bis(biphenylene)methyl linkers, are prepared. Although the presence of slow interconversion (on the NMR time scale) between significantly populated conformers may not be strictly excluded, most likely the polyethers are mixtures of diastereomers (with nearly coincident NMR chemical shifts). Radii of gyration for polyethers in tetrahydrofuran- $d_8$  are in the 1.2–1.8 nm range. The corresponding polyradicals are likely to possess sizes similar to those of polyethers.<sup>1</sup>

Polyradicals possess relatively large values of average  $S$ ; the value  $S \approx 13$  for the branched 36-radical **4** is the highest among organic molecules. Notably, the values of  $S$  increase with the increasing number of the  $S = 1/2$  radicals (triarylmethyls). Pentadecaradical **2** and 22-radical **3**, in which macrocyclic modules are connected with bis(biphenylene)methyl linkers in a quasilinear fashion, provide excellent model compounds for unequal-spin clusters with random distribution of ferromagnetic and antiferromagnetic couplings. Because polyradicals **2–4** may be viewed as linear and branched fragments of the first conjugated polymer with magnetic ordering, our analyses of magnetic data for **2** and **3** may provide a rationale for extraordinary extent of net ferromagnetic exchange couplings leading to high values of magnetic moment (or  $S$ ) in such polymers.

### Experimental Section

**Macrocyclic Modules: 11A, 11B, 11C, and 11D.** A round-bottom flask with sidearm was charged with NaH (0.12 g of 60% dispersion in mineral oil, 3.0 mmol). After removal of the mineral oil with pentane under nitrogen flow, THF (2.0 mL) was added, and then, during cooling with an ice bath, macrocyclic diol **10A** (0.541 g, 0.272 mmol) in THF (4.0 mL) was added. The resultant suspension was stirred for 2 h, during which time the temperature of cooling bath was allowed to reach ambient temperature. After the bath was recooled to 0 °C, MeI (0.30 mL, 4.817 mmol) was added. Following 20 h of stirring at ambient temperature, aqueous workup was carried out. After extraction with ether, the organic layer was dried over MgSO<sub>4</sub> and concentrated in vacuo to give a light yellow solid. Column chromatography (flash silica gel, 3–5% ether in hexane) gave 249 mg (45%) of clear solid, which was used for the next step (softened at 139 °C and melted at 164–166 °C). From four other reactions on the 0.9, 0.56, 0.25, and 0.1 g scales, 0.836 g (44–57%) of macrocyclic module **11A** was isolated from 1.841 g of macrocyclic diol **10A**. Starting from macrocyclic diol **10B** (0.365 g), module **11B** (0.218 g, 59%) was obtained. Overall, from five reactions on the 1.5, 0.7 (2), 0.4 (2) g scales, 1.505 g (40%) of module **10B** was isolated from 3.687 g of **10B**. From two reactions on the 0.5 and 0.1 g scales, 0.198 g (33%) of module **10B** was isolated. From two reactions, starting from 0.8148 g of impure **10A**, 0.0268 g (3%) of module **11D** was also isolated.

**Module 11A.** Anal. Calcd for C<sub>138</sub>H<sub>163</sub>O<sub>7</sub>Br: C, 82.31; H, 8.16. Found: 82.59; H, 7.96. IR (cm<sup>-1</sup>): 1595 (Ar), 1085 (C–O–C). FABMS (3-NBA) cluster:  $m/z$  (% RA for  $m/z = 400–2140$ ) at ( $M - OCH_3$ )<sup>+</sup> 1980.0 (62), 1981.0 (81), 1982.0 (100), 1983.0 (83), 1984.0 (55), 1985.0 (27); calcd for C<sub>137</sub>H<sub>160</sub>O<sub>6</sub>Br at ( $M - OCH_3$ )<sup>+</sup> 1980.1 (46), 1981.1 (71), 1982.1 (100), 1983.1 (98), 1984.1 (65), 1985.1 (32), 1986.1 (12). <sup>1</sup>H NMR (500 MHz, EM = -1.50, GB = 0.80, C<sub>6</sub>D<sub>6</sub>, 293 K, <sup>1</sup>H–<sup>1</sup>H COSY cross-peaks in aromatic region): 1,3,5-Trisubstituted benzene rings (rings A, A', B, C): Rings A, A': 8.202 (t,  $J = 2$ , 2 H,

7.821, 7.297), 7.821 (t,  $J = 2$ , 2 H, 8.202, 7.297), 7.297 (t,  $J = 2$ , 2 H, 8.202, 7.821). Rings B and C: 7.775 (t,  $J = 2$ , 1 H, 7.650), 7.650 (d,  $J = 2$ , 2 H, 7.775), 7.770 (d,  $J = 1.5$ , 2 H, 7.734), 7.734 (br, 1 H, 7.770). 1,4-Disubstituted benzene rings 1,1'-5,5': 7.565 (d,  $J = 9$ , 4 H, 7.271), 7.271 (d,  $J = 9$ , 4 H, 7.565); 7.542 (d,  $J = 9$ , 4 H, 7.211), 7.211 (d,  $J = 9$ , 4 H, 7.542); 7.443 (d,  $J = 8$ , 4 H, 7.261), 7.261 (d,  $J = 9$ , 4 H, 7.443); 7.389 (d,  $J = 8$ , 4 H, 7.189), 7.189 (d,  $J = 8$ , 4 H, 7.389); 7.335 (d,  $J = 8$ , 4 H, 7.201), 7.201 (d,  $J = 9$ , 4 H, 7.335). Aliphatic region: 3.016 (s, 6 H), 2.914 (s, 3 H), 2.883 (s, 6 H), 2.776 (s, 6 H), 1.264 (s, 18 H), 1.242 (s, 18 H), 1.223 (s, 18 H), 1.221 (s, 18 H), 1.187 (s, 18 H). <sup>1</sup>H NMR (500 MHz, C<sub>6</sub>D<sub>6</sub>, 328 K): 8.20–7.10 (m, 52 H), 3.015 (s, 6 H), 2.919 (s, 3 H), 2.901 (s, 6 H), 2.812 (s, 6 H), 1.228 (s, 18 H), 1.222 (s, 18 H), 1.213 (s, 36 H), 1.192 (s, 18 H). <sup>1</sup>H NMR (500 MHz, C<sub>6</sub>D<sub>6</sub>, 348 K): 8.20–7.10 (m, 52 H), 3.017 (s, 6 H), 2.921 (s, 3 H), 2.909 (s, 6 H), 2.830 (s, 6 H), 1.232 (s, 18 H), 1.225 (s, 18 H), 1.219 (s, 36 H), 1.198 (s, 18 H). <sup>13</sup>C{<sup>1</sup>H}DEPT(135°)-NMR (125 MHz, EM = -1.30, GB = 0.90, C<sub>6</sub>D<sub>6</sub>, 293 K): aromatic quaternary region, expected, 17 resonances; found, 17 resonances at 150.3 (q), 150.0 (q), 149.9 (q), 149.81 (q), 149.74 (q), 148.7 (q), 145.1 (q), 144.5 (q), 143.6 (q), 142.92 (q), 142.86 (q), 142.56 (q), 142.51 (q), 142.4 (q), 141.2 (q), 140.6 (q), 122.3 (q); aromatic nonquaternary region, expected, 17 resonances; found 13 resonances at 130.2, 129.89, 129.88, 129.6, 129.5, 129.37, 129.32, 128.0, 127.3, 125.31, 125.26, 125.24, 125.1; aliphatic region, 88.0 (q), 87.8 (q), 87.61 (q), 87.57 (q), 52.59, 52.51, 52.47, 52.3, 34.79 (q), 34.75 (q), 31.85, 31.81.

**Module 11B.** Clear solid (softened at 177 °C and melted at 183–185 °C). Anal. Calcd for C<sub>138</sub>H<sub>163</sub>O<sub>7</sub>Br: C, 82.31; H, 8.16. Found: 82.41; H, 8.33. IR (cm<sup>-1</sup>): 1594 (Ar), 1082 (C–O–C). FABMS (3-NBA) cluster:  $m/z$  (% RA for  $m/z = 400–2440$ ) at ( $M - OCH_3$ )<sup>+</sup> 1980.0 (63), 1981.0 (81), 1982.0 (100), 1983.0 (90), 1984.0 (58), 1985.0 (28); calcd for C<sub>137</sub>H<sub>160</sub>O<sub>6</sub>Br at ( $M - OCH_3$ )<sup>+</sup> 1980.1 (46), 1981.1 (71), 1982.1 (100), 1983.1 (98), 1984.1 (65), 1985.1 (32), 1986.1 (12). <sup>1</sup>H NMR (500 MHz, EM = -1.80, GB = 0.80, C<sub>6</sub>D<sub>6</sub>, 293 K, <sup>1</sup>H–<sup>1</sup>H COSY cross-peaks in aromatic region): 1,3,5-Trisubstituted benzene rings (rings A – D): Ring A: 8.177 (t,  $J = 2$ , 1 H, 7.791, 7.448), 7.791 (t,  $J = 2$ , 1 H, 8.177, 7.448), 7.448 (t,  $J = 2$ , 1 H, 8.177, 7.791). Ring B: 8.120 (t,  $J = 2$ , 1 H, 7.642, 7.504), 7.642 (t,  $J = 2$ , 1 H, 8.120, 7.504), 7.504 (t,  $J = 2$ , 1 H, 8.120, 7.642). Ring C: 7.859 (t,  $J = 2$ , 1 H, 7.822, 7.752), 7.822 (t,  $J = 2$ , 1 H, 7.859, 7.752), 7.752 (t,  $J = 2$ , 1 H, 7.859, 7.822). Ring D: 7.781 (t,  $J = 2$ , 1 H, 7.759, 7.672), 7.759 (t,  $J = 2$ , 1 H, 7.781, 7.672), 7.672 (t,  $J = 2$ , 1 H, 7.781, 7.759). 1,4-Disubstituted benzene rings 1–10: 7.548 (d,  $J = 9$ , 2 H, 7.232), 7.232 (d,  $J = 9$ , 2 H, 7.548); 7.547 (d,  $J = 9$ , 2 H, 7.269), 7.269 (d,  $J = 9$ , 2 H, 7.547); 7.501 (d,  $J = 9$ , 2 H, 7.366), 7.366 (d,  $J = 9$ , 2 H, 7.501); 7.458 (d,  $J = 9$ , 2 H, 7.180), 7.180 (d,  $J = 9$ , 2 H, 7.458); 7.452 (d,  $J = 9$ , 2 H, 7.226), 7.226 (d,  $J = 9$ , 2 H, 7.452); 7.452 (d,  $J = 9$ , 2 H, 7.206), 7.206 (d,  $J = 9$ , 2 H, 7.452); 7.426 (d,  $J = 9$ , 2 H, 7.206), 7.206 (d,  $J = 9$ , 2 H, 7.426); 7.405 (d,  $J = 9$ , 2 H, 7.134), 7.134 (d,  $J = 9$ , 2 H, 7.405); 7.402 (d,  $J = 9$ , 2 H, 7.179), 7.179 (d,  $J = 9$ , 2 H, 7.402); 7.371 (d,  $J = 9$ , 2 H, 7.142), 7.142 (d,  $J = 9$ , 2 H, 7.371). Aliphatic region: 3.028 (s, 3 H), 2.982 (s, 3 H), 2.925 (s, 3 H), 2.914 (s, 3 H), 2.858 (s, 3 H), 2.812 (s, 3 H), 2.775 (s, 3 H), 1.239 (s, 9 H), 1.217 (s, 9 H), 1.215 (s, 9 H), 1.212 (s, 9 H), 1.201 (s, 9 H), 1.199 (s, 9 H), 1.197 (s, 9 H), 1.190 (s, 9 H), 1.161 (s, 9 H), 1.153 (s, 9 H). <sup>1</sup>H NMR (500 MHz, EM = -1.70, GB = 0.80, C<sub>6</sub>D<sub>6</sub>, 328 K): 8.20–7.10 (m, 52 H), 3.024 (s, 3 H), 2.980 (s, 3 H), 2.928 (s, 3 H), 2.910 (s, 3 H), 2.868 (s, 3 H), 2.819 (s, 3 H), 2.785 (s, 3 H), 1.239 (s, 9 H), 1.219 (s, 9 H), 1.213 (s, 18 H), 1.202 (s, 9 H), 1.199 (s, 9 H), 1.197 (s, 9 H), 1.191 (s, 9 H), 1.161 (s, 9 H), 1.154 (s, 9 H). <sup>1</sup>H NMR (500 MHz, EM = -1.80, GB = 0.80, C<sub>6</sub>D<sub>6</sub>, 348 K, <sup>1</sup>H–<sup>1</sup>H COSY cross-peaks in aromatic region): 1,3,5-Trisubstituted benzene rings (rings A – D): Ring A: 8.045 (t,  $J = 2$ , 1 H, 7.712, 7.378), 7.712 (t,  $J = 2$ , 1 H, 8.045, 7.378), 7.378 (t,  $J = 2$ , 1 H, 8.045, 7.712). Ring B: 7.998 (t,  $J = 2$ , 1 H, 7.618, 7.435), 7.618 (t,  $J = 2$ , 1 H, 7.998, 7.435), 7.435 (t,  $J = 2$ , 1 H, 7.998, 7.618). Ring C: 7.791 (t,  $J = 2$ , 1 H, 7.756, 7.666), 7.666 (t,  $J = 2$ , 1 H, 7.791, 7.756), 7.756 (t,  $J = 2$ , 1 H,

7.791, 7.666). Ring D: 7.720 (t,  $J = 2$ , 1 H, 7.645, 7.615), 7.645 (t,  $J = 2$ , 1 H, 7.720, 7.615), 7.615 (t,  $J = 2$ , 1 H, 7.720, 7.645). 1,4-Disubstituted benzene rings 1–10: 7.492 (d,  $J = 9$ , 2 H, 7.221), 7.221 (d,  $J = 9$ , 2 H, 7.492); 7.490 (d,  $J = 9$ , 2 H, 7.252), 7.252 (d,  $J = 9$ , 2 H, 7.490); 7.429 (d,  $J = 9$ , 2 H, 7.317), 7.317 (d,  $J = 9$ , 2 H, 7.429); 7.429 (d,  $J = 9$ , 2 H, 7.205), 7.205 (d,  $J = 9$ , 2 H, 7.429); 7.403 (d,  $J = 9$ , 2 H, 7.226), 7.226 (d,  $J = 9$ , 2 H, 7.403); 7.380 (d,  $J = 9$ , 2 H, 7.198), 7.198 (d,  $J = 9$ , 2 H, 7.380); 7.386–7.353 (m, 8 H, 7.196–7.133), 7.196–7.133 (m, 8 H, 7.386–7.353). Aliphatic region: 3.012 (s, 3 H), 2.974 (s, 3 H), 2.932 (s, 3 H), 2.901 (s, 3 H), 2.892 (s, 3 H), 2.844 (s, 3 H), 2.810 (s, 3 H), 1.239 (s, 9 H), 1.224 (s, 9 H), 1.212 (s, 9 H), 1.206 (s, 9 H), 1.205 (s, 9 H), 1.199 (s, 9 H), 1.197 (s, 9 H), 1.192 (s, 9 H), 1.160 (s, 9 H), 1.157 (s, 9 H).  $^{13}\text{C}\{^1\text{H}\}$ -DEPT(135°)NMR (125 MHz, EM = -1.20, GB = 0.80,  $\text{C}_6\text{D}_6$ , 293 K): aromatic quaternary region, expected, 32 resonances; found, 29 resonances at 150.5 (q), 150.2 (q), 150.00 (q), 149.97 (q), 149.92 (q), 149.80 (q), 149.75 (q), 149.66 (q), 149.0 (q), 148.6 (q), 145.8 (q), 144.7 (q), 144.3 (q), 143.81 (q), 143.79 (q), 143.67 (q), 143.2 (q), 143.1 (q), 143.0 (q), 142.7 (q), 142.4 (q), 142.17 (q), 142.16 (q), 142.0 (q), 141.9 (q), 141.6 (q), 141.1 (q), 140.4 (q), 122.5 (q); aromatic nonquaternary region, expected, 32 resonances; found 21 resonances at 130.16, 130.07, 130.05, 129.98, 129.82, 129.79, 129.67, 129.60, 129.57, 129.53, 129.46, 129.41, 129.13, 129.04, 126.6, 125.43, 125.32, 125.26, 125.17, 125.13, 125.07; aliphatic region, 88.2 (q), 87.81 (q), 87.70 (q), 87.65 (q), 82.63 (q), 52.8, 52.54, 52.52, 52.51, 52.49, 52.47, 34.83 (q), 34.79 (q), 34.76 (q), 34.74 (q), 31.88, 31.86, 31.82, 31.78, 31.74.

**Module 11C.** This  $C_1$ -symmetric isomer is not pure; extra peaks in the  $^1\text{H}$  and  $^{13}\text{C}$  NMR spectra are found. Clear solid (softened at 184 °C and melted at 189–191 °C). Anal. Calcd for  $\text{C}_{138}\text{H}_{163}\text{O}_7\text{Br}$ : C, 82.31; H, 8.16. Found: 82.41; H, 8.33. IR ( $\text{cm}^{-1}$ ): 1594 (Ar), 1083 (C–O–C). FABMS (3-NBA) cluster:  $m/z$  (% RA for  $m/z = 320$ –2440) at ( $M - \text{OCH}_3$ ) $^+$  1980.0 (61), 1981.0 (86), 1982.0 (100), 1983.0 (84), 1984.0 (57), 1985.0 (27); calcd for  $\text{C}_{137}\text{H}_{160}\text{O}_6\text{Br}$  at ( $M - \text{OCH}_3$ ) $^+$  1980.1 (46), 1981.1 (71), 1982.1 (100), 1983.1 (98), 1984.1 (65), 1985.1 (32).  $^1\text{H}$  NMR (500 MHz, EM = -1.00, GB = 0.44,  $\text{C}_6\text{D}_6$ , 298 K): 8.20–7.10 (m, 52 H), 3.017 (s, 3 H), 2.990 (s, 3 H), 2.953 (s, 3 H), 2.882 (s, 3 H), 2.872 (s, 3 H), 2.782 (s, 3 H), 2.735 (s, 3 H), 1.224 (s, 9 H), 1.208 (s, 9 H), 1.205 (s, 9 H), 1.201 (s, 9 H), 1.196 (s, 9 H), 1.189 (s, 9 H), 1.186 (s, 9 H), 1.181 (s, 9 H), 1.178 (s, 9 H), 1.157 (s, 9 H).  $^1\text{H}$  NMR (500 MHz, EM = -0.84, GB = 0.44,  $\text{C}_6\text{D}_6$ , 328 K,  $^1\text{H}$ – $^1\text{H}$  COSY cross-peaks in aromatic region): 1,3,5-Trisubstituted benzene rings (rings A – D): Ring A: 7.938 (t,  $J = 2$ , 1 H, 7.891, 7.488), 7.891 (t,  $J = 2$ , 1 H, 7.938, 7.488), 7.488 (t,  $J = 2$ , 1 H, 7.938, 7.891). Ring B: 7.904 (t,  $J = 2$ , 1 H, 7.776, 7.628), 7.776 (t,  $J = 2$ , 1 H, 7.904, 7.628), 7.628 (t,  $J = 2$ , 1 H, 7.904, 7.776). Ring C: 7.891 (t,  $J = 2$ , 1 H, 7.695, 7.688), 7.695 (t,  $J = 2$ , 1 H, 7.891, 7.688), 7.688 (t,  $J = 2$ , 1 H, 7.891, 7.695). Ring D: 7.815 (t,  $J = 2$ , 1 H, 7.797, 7.536), 7.797 (t,  $J = 2$ , 1 H, 7.815, 7.536), 7.536 (t,  $J = 2$ , 1 H, 7.815, 7.797). 1,4-Disubstituted benzene rings 1–10: 7.526 (d,  $J = 9$ , 2 H, 7.233), 7.233 (d,  $J = 9$ , 2 H, 7.526); 7.515 (d,  $J = 9$ , 2 H, 7.215), 7.215 (d,  $J = 9$ , 2 H, 7.515); 7.511 (d,  $J = 9$ , 2 H, 7.252), 7.252 (d,  $J = 9$ , 2 H, 7.511); 7.496 (d,  $J = 9$ , 2 H, 7.240), 7.240 (d,  $J = 9$ , 2 H, 7.496); 7.482 (d,  $J = 9$ , 2 H, 7.250), 7.250 (d,  $J = 9$ , 2 H, 7.482); 7.453 (d,  $J = 9$ , 2 H, 7.209), 7.209 (d,  $J = 9$ , 2 H, 7.453); 7.437 (d,  $J = 9$ , 2 H, 7.208), 7.208 (d,  $J = 9$ , 2 H, 7.437); 7.411 (d,  $J = 9$ , 2 H, 7.220), 7.220 (d,  $J = 9$ , 2 H, 7.411); 7.385 (d,  $J = 9$ , 2 H, 7.248), 7.248 (d,  $J = 9$ , 2 H, 7.385); 7.362 (d,  $J = 9$ , 2 H, 7.167), 7.167 (d,  $J = 9$ , 2 H, 7.362). Aliphatic region: 3.010 (s, 3 H), 2.982 (s, 3 H), 2.955 (s, 3 H), 2.893 (s, 3 H), 2.886 (s, 3 H), 2.824 (s, 3 H), 2.769 (s, 3 H), 1.231 (s, 9 H), 1.217 (s, 9 H), 1.216 (s, 9 H), 1.210 (s, 9 H), 1.207 (s, 9 H), 1.198 (s, 18 H), 1.194 (s, 9 H), 1.192 (s, 9 H), 1.177 (s, 9 H).  $^1\text{H}$  NMR (500 MHz, EM = -0.51, GB = 0.47,  $\text{C}_6\text{D}_6$ , 348 K,  $^1\text{H}$ – $^1\text{H}$  COSY cross-peaks in aromatic region): 1,3,5-Trisubstituted benzene rings (rings A – D): Ring A: 7.892 (t,  $J = 2$ , 1 H, 7.857, 7.454), 7.857 (t,  $J = 2$ , 1 H, 8.045, 7.454), 7.454 (t,  $J = 2$ , 1 H, 7.892, 7.857). Ring B: 7.866 (t,  $J = 2$ , 1 H, 7.737, 7.601), 7.737 (t,  $J = 2$ , 1 H, 7.866, 7.601),

7.601 (t,  $J = 2$ , 1 H, 7.866, 7.737). Ring C: 7.840 (t,  $J = 2$ , 1 H, 7.691, 7.682), 7.691 (t,  $J = 2$ , 1 H, 7.840, 7.682), 7.682 (t,  $J = 2$ , 1 H, 7.840, 7.691). Ring D: 7.791 (t,  $J = 2$ , 1 H, 7.770, 7.516), 7.770 (t,  $J = 2$ , 1 H, 7.791, 7.516), 7.516 (t,  $J = 2$ , 1 H, 7.770, 7.645). 1,4-Disubstituted benzene rings 1–10: 7.506 (d,  $J = 8$ , 2 H, 7.233), 7.233 (d,  $J = 9$ , 2 H, 7.506); 7.489 (d,  $J = 9$ , 2 H, 7.215), 7.215 (d,  $J = 9$ , 2 H, 7.489); 7.488 (d,  $J = 9$ , 2 H, 7.252), 7.252 (d,  $J = 9$ , 2 H, 7.488); 7.469 (d,  $J = 9$ , 2 H, 7.240), 7.240 (d,  $J = 9$ , 2 H, 7.469); 7.458 (d,  $J = 9$ , 2 H, 7.250), 7.250 (d,  $J = 8$ , 2 H, 7.458); 7.442 (d,  $J = 9$ , 2 H, 7.209), 7.209 (d,  $J = 9$ , 2 H, 7.442); 7.426 (d,  $J = 9$ , 2 H, 7.208), 7.208 (d,  $J = 9$ , 2 H, 7.426); 7.397 (d,  $J = 9$ , 2 H, 7.220), 7.220 (d,  $J = 9$ , 2 H, 7.397); 7.369 (d,  $J = 9$ , 2 H, 7.248), 7.248 (d,  $J = 8$ , 2 H, 7.369); 7.355 (d,  $J = 9$ , 2 H, 7.167), 7.167 (d,  $J = 9$ , 2 H, 7.355). Aliphatic region: 3.008 (s, 3 H), 2.978 (s, 3 H), 2.959 (s, 3 H), 2.900 (s, 3 H), 2.895 (s, 3 H), 2.850 (s, 3 H), 2.785 (s, 3 H), 1.240 (s, 9 H), 1.225 (s, 9 H), 1.221 (s, 9 H), 1.218 (s, 9 H), 1.212 (s, 9 H), 1.205 (s, 27 H), 1.200 (s, 9 H), 1.189 (s, 9 H).  $^{13}\text{C}\{^1\text{H}\}$ DEPT(135°)-NMR (125 MHz,  $\text{C}_6\text{D}_6$ , 293 K): aromatic quaternary region, expected, 32 resonances; found, 28 resonances at 150.5 (q), 150.4 (q), 150.2 (q), 149.94 (q), 149.87 (q), 149.81 (q), 149.7 (q), 149.6 (q), 147.9 (q), 145.0 (q), 144.55 (q), 144.45 (q), 144.41 (q), 143.8 (q), 143.7 (q), 143.51 (q), 143.47 (q), 143.38 (q), 143.0 (q), 142.9 (q), 142.79 (q), 142.69 (q), 142.4 (q), 142.0 (q), 140.9 (q), 140.5 (q), 140.3 (q), 122.2 (q); aromatic nonquaternary region, expected, 32 resonances; found 23 resonances at 131.1, 130.9, 130.3, 130.0, 129.8, 129.6, 129.52, 129.48, 129.41, 129.36, 129.18, 129.16, 129.11, 128.85, 128.76 ( $\text{C}_6\text{D}_5\text{H}$ ), 128.68, 128.23, 128.18, 127.5, 125.4, 125.23, 125.20, 125.17, 125.0; aliphatic region, 88.23 (q), 88.15 (q), 87.84 (q), 87.75 (q), 87.71 (q), 87.62 (q), 52.68, 52.64, 52.59, 52.55, 52.49, 52.39, 34.84 (q), 34.80 (q), 34.77 (q), 31.85, 31.82, 31.78.

**Module 11D.** This  $C_2$ -symmetric isomer is not pure; additional peaks in the  $^1\text{H}$  and  $^{13}\text{C}$  NMR spectra are found. Yellow solid (softened at 100 °C and melted at 113–115 °C). IR ( $\text{cm}^{-1}$ ): 1594 (Ar), 1082 (C–O–C). FABMS (3-NBA) cluster:  $m/z$  (% RA for  $m/z = 400$ –2140) at ( $M - \text{OCH}_3$ ) $^+$  1980.0 (65), 1981.0 (79), 1982.0 (100), 1983.0 (87), 1984.0 (61), 1985.0 (28); calcd for  $\text{C}_{137}\text{H}_{160}\text{O}_6\text{Br}$  at ( $M - \text{OCH}_3$ ) $^+$ : 1980.1 (46), 1981.1 (71), 1982.1 (100), 1983.1 (98), 1984.1 (65), 1985.1 (32), 1986.1 (12).  $^1\text{H}$  NMR (500 MHz, EM = -1.80, GB = 0.80,  $\text{C}_6\text{D}_6$ , 293 K,  $^1\text{H}$ – $^1\text{H}$  COSY cross-peaks in aromatic region): 1,3,5-Trisubstituted benzene rings (rings A, A', B, C): Rings A, A': 8.008 (t,  $J = 2$ , 2 H, 7.767, 7.581), 7.767 (t,  $J = 2$ , 2 H, 8.008, 7.581), 7.581 (t,  $J = 2$ , 2 H, 8.008, 7.767). Rings B and C: 7.878 (t,  $J = 1.5$ , 1 H, 7.736), 7.736 (d,  $J = 1.5$ , 2 H, 7.878), 7.871 (t,  $J = 2$ , 1 H, 7.794), 7.794 (d,  $J = 2$ , 2 H, 7.871). 1,4-Disubstituted benzene rings 1,1'-5,5': 7.530 (d,  $J = 9$ , 4 H, 7.222), 7.222 (d,  $J = 8$ , 4 H, 7.530); 7.491 (d,  $J = 8$ , 4 H, 7.212), 7.212 (d,  $J = 9$ , 4 H, 7.491); 7.478 (d,  $J = 8$ , 2 H, 7.182), 7.182 (d,  $J = 9$ , 2 H, 7.478) (diastereotopic); 7.467 (d,  $J = 8$ , 4 H, 7.236), 7.236 (d,  $J = 8$ , 4 H, 7.467); 7.446 (d,  $J = 8$ , 4 H, 7.180), 7.180 (d,  $J = 8$ , 4 H, 7.446); 7.414 (d,  $J = 9$ , 2 H, 7.194), 7.194 (d,  $J = 9$ , 2 H, 7.414) (diastereotopic). Aliphatic region: 2.950 (s, 6 H), 2.942 (s, 6 H), 2.840 (s, 3 H), 2.807 (s, 6 H), 1.208 (s, 18 H), 1.196 (s, 27 H), 1.180 (s, 18 H), 1.156 (s, 18 H), 1.146 (s, 9 H).  $^{13}\text{C}\{^1\text{H}\}$ DEPT(135°)NMR (125 MHz, EM = -0.30, GB = 0.50,  $\text{C}_6\text{D}_6$ , 293 K): aromatic quaternary region, expected, 19 resonances; found, 19 resonances at 150.5 (q), 150.0 (q), 149.9 (q), 149.8 (q), 149.57 (q), 149.54 (q), 148.6 (q), 144.40 (q), 144.35 (q), 143.8 (q), 143.3 (q), 143.09 (q), 142.96 (q), 142.64 (q), 142.59 (q), 142.3 (q), 142.0 (q), 140.6 (q), 122.5 (q); aromatic nonquaternary region, expected, 19 resonances; found 18 resonances at 129.92, 129.89, 129.84, 129.7, 129.34, 129.31, 129.24, 129.16, 128.5, 129.0, 128.8, 128.7, 127.4, 126.4, 125.4, 125.24, 125.21, 125.1; aliphatic region, 88.2 (q), 87.70 (q), 87.64 (q), 87.56 (q), 52.8, 52.48, 52.46, 52.41, 34.79 (q), 34.77 (q), 34.75 (q), 34.70 (q), 31.85, 31.83, 31.81, 31.72.

**Module-with-Linker: 15A and 15B.** *t*-BuLi (0.172 mL of a ~1.5 M solution in pentane, 0.26 mmol, Acros) was added to a solution of module 11A (0.238 g, 0.118 mmol) in THF (1.40 mL) in a heavy-wall

Schlenk vessel at  $-78\text{ }^{\circ}\text{C}$ . After 3 h, the reaction mixture was warmed to  $-20\text{ }^{\circ}\text{C}$  for 10 min and then re-cooled to  $-78\text{ }^{\circ}\text{C}$ . Following addition of  $\text{ZnCl}_2$  (0.166 mL of 0.81 M solution in ether, 0.134 mmol), the reaction mixture was allowed to attain ambient temperature for 2 h. The resultant clear light orange solution was transferred to a glovebox.  $\text{Pd}(\text{PPh}_3)_4$  (4.0 mg, 0.0035 mmol) and racemic linker **14** (0.127 mg, 0.236 mmol) were added to the reaction mixture. Subsequently, the reaction mixture was heated in an oil bath at  $100\text{ }^{\circ}\text{C}$  for 1.5 days. After extraction with ether, the organic layer was dried over  $\text{MgSO}_4$  and concentrated in vacuo to give a yellow solid. Column chromatography (TLC grade silica gel, 3–5% ether in hexane), followed by the treatment with ether/MeOH, gave 0.145 mg (52%) of module-with-linker **15A** as a white powder (softening to clear solid at  $209\text{--}211\text{ }^{\circ}\text{C}$ ). From two other reactions on the 0.3 and 0.3 g scales, 0.338 g (39–59%) of module-with-linker **15A** was obtained from 0.597 g of module **11A**. Module-with-linker **15B** (0.386 mg, 58%) was obtained as white powder (softening to clear solid at  $203\text{--}205\text{ }^{\circ}\text{C}$ ), starting from 0.572 g of module **11B**. From another reaction, 0.323 g (56%) of **15B** was obtained from 0.493 g of module **11B**.

**Module-with-Linker 15A.** Calcd for  $\text{C}_{162}\text{H}_{187}\text{O}_8\text{Br}$ : C, 83.08; H, 8.05. Found: 83.56; H, 8.47. IR ( $\text{cm}^{-1}$ ): 1593 (Ar), 1083 (C–O–C). FABMS (3-NBA) cluster:  $m/z$  (% RA for  $m/z = 480\text{--}3000$ ) at  $(M - \text{OCH}_3)^+$ : 2308.2 (52), 2309.2 (81), 2310.2 (99), 2311.2 (100), 2312.2 (78), 2313.4 (39), 2314.4 (21); calcd for  $\text{C}_{161}\text{H}_{184}\text{O}_7\text{Br}$  at  $(M - \text{OCH}_3)^+$ : 2308.3 (36), 2309.3 (65), 2310.3 (95), 2311.3 (100), 2312.3 (75), 2313.3 (42), 2314.3 (18), 2315.3 (6).  $^1\text{H}$  NMR (500 MHz, EM =  $-1.40\text{--}2.20$ , GB = 0.80/0.90,  $\text{C}_6\text{D}_6$ , 293 K,  $^1\text{H}\text{--}^1\text{H}$  COSY cross-peaks in aromatic region): Rings A, A': 8.097, 8.094 (t, t,  $J = 2$ ,  $J = 2$ , 2 H, [7.974, 7.971], 7.490), 7.974, 7.971 (t, t,  $J = 2$ ,  $J = 2$ , 2 H, [8.097, 8.094], 7.490), 7.490 (t,  $J = 2$ , 2 H, [8.097, 8.094], 7.974). Rings B and C: 7.924 (d,  $J = 2$ , 2 H, 7.836), 7.836 (br, 1 H, 7.924); 7.877 (t,  $J = 2$ , 1 H, 7.631), 7.631 (d,  $J = 2$ , 2 H, 7.877). Rings 1,1'-5,5': 7.579 (d,  $J = 9$ , 4 H, 7.250), 7.250 (d,  $J = 9$ , 4 H, 7.579); 7.555 (d,  $J = 8$ , 4 H, 7.190), 7.190 (d,  $J = 9$ , 4 H, 7.555); 7.488 (d,  $J = 9$ , 4 H, 7.215), 7.215 (d,  $J = 9$ , 4 H, 7.488); 7.442 (d,  $J = 9$ , 4 H, 7.211), 7.211 (d,  $J = 9$ , 4 H, 7.442); 7.375 (d,  $J = 8$ , 4 H, 7.151), 7.151 (d,  $J = 9$ , 4 H, 7.375). Rings 6–8: 7.399 (d,  $J = 8$ , 2 H, 7.280), 7.280 (d,  $J = 8$ , 2 H, 7.399); 7.375 (d,  $J = 9$ , 2 H, 7.272), 7.272 (d,  $J = 9$ , 2 H, 7.375); 7.247 (s, 4 H); overlapped AB system. Aliphatic region: 2.982, 2.980 (s, s, 3 H), 2.980 (s, 3 H), 2.917 (s, 6 H), 2.906 (s, 3 H), 2.886 (s, 3 H), 2.850 (s, 6 H), 1.223 (s, 9 H), 1.205 (s, 18 H), 1.192 (s, 9 H), 1.191 (s, 9 H), 1.189 (s, 18 H), 1.179 (s, 18 H), 1.160 (s, 18 H).  $^{13}\text{C}\{^1\text{H}\}$ DEPT(135 $^{\circ}$ )NMR (125 MHz, EM =  $-1.00$ , GB = 0.80,  $\text{C}_6\text{D}_6$ , 293 K): aromatic quaternary region, expected, 23 resonances; found, 22 resonances at 150.4 (q), 150.1 (q), 150.0 (q), 149.88 (q), 149.77 (q), 149.71 (q), 146.4 (q), 145.0 (q), 144.7, 143.6 (q), 143.4 (q), 143.1 (q), 142.77 (q), 142.68 (q), 142.66 (q), 142.5 (q), 141.6 (q), 141.27 (q), 141.22 (q), 140.9 (q), 140.2 (q), 121.6 (q); aromatic nonquaternary region, expected, 23 resonances; found 18 resonances at 131.5, 131.0, 130.04, 129.96, 129.6, 129.5, 129.38, 129.34, 129.30, 128.8 ( $\text{C}_6\text{D}_5\text{H}$ ), 128.0, 127.2, 126.3, 125.4, 125.26, 125.21, 125.18, 125.16, 125.0; aliphatic region, 88.2 (q), 88.1 (q), 87.9 (q), 87.6 (q), 87.1 (q), 52.6, 52.53, 52.51, 52.3, 34.81 (q), 34.79 (q), 34.77 (q), 34.74 (q), 31.87, 31.85, 31.83, 31.81, 31.79.

**Module-with-Linker 15B.** Calcd for  $\text{C}_{162}\text{H}_{187}\text{O}_8\text{Br}$ : C, 83.08; H, 8.05. Found: 83.61; H, 7.72. Found: 81.88; H, 7.72. IR ( $\text{cm}^{-1}$ ): 1594 (Ar), 1081 (C–O–C). FABMS (3-NBA) cluster:  $m/z$  (% RA for  $m/z = 480\text{--}3000$ ) at  $(M - \text{OCH}_3)^+$ : 2308.2 (58), 2309.2 (82), 2310.3 (100), 2311.3 (97), 2312.5 (76), 2313.4 (39), 2314.4 (21); calcd for  $\text{C}_{161}\text{H}_{184}\text{O}_7\text{Br}$  at  $(M - \text{OCH}_3)^+$ : 2308.3 (36), 2309.3 (65), 2310.3 (95), 2311.3 (100), 2312.3 (75), 2313.3 (42), 2314.3 (18), 2315.3 (6).  $^1\text{H}$  NMR (500 MHz, EM =  $-1.80$ , GB = 0.80,  $\text{C}_6\text{D}_6$ , 293 K,  $^1\text{H}\text{--}^1\text{H}$  COSY cross-peaks in aromatic region): Rings A: 8.110 (t,  $J = 2$ , 1 H, 7.887, 7.616), 7.887 (t,  $J = 2$ , 1 H, 8.110, 7.616), 7.616 (t,  $J = 2$ , 1 H, 8.110, 7.887). Rings B: 8.022 (br, 1 H, 7.768, 7.692), 7.768 (br, 1 H, 8.022, 7.692), 7.692 (br, 1 H, 8.022, 7.768). Rings C: 7.979,

7.977 (t, t,  $J = 2$ ,  $J = 2$ , 1 H, 7.094, [7.869, 7.866]), 7.094 (br, 1 H, [7.979, 7.977], [7.869, 7.866]), 7.869, 7.866 (t, t,  $J = 2$ ,  $J = 2$ , 1 H, [7.979, 7.977], 7.094). Ring D: 7.794, 7.790 (t, t,  $J = 2$ ,  $J = 2$ , 1 H, [7.767, 7.763]), [7.686, 7.683]), 7.767, 7.763 (t, t,  $J = 2$ ,  $J = 2$ , 1 H, [7.794, 7.790]), [7.686, 7.683]), [7.686, 7.683]), 7.686, 7.683 (t, t,  $J = 2$ ,  $J = 2$ , 1 H, [7.794, 7.790]), [7.767, 7.763]). Rings 1–13: 7.591 (d,  $J = 9$ , 2 H, 7.207), 7.207 (d,  $J = 9$ , 2 H, 7.591); 7.556 (d,  $J = 9$ , 2 H, 7.225), 7.225 (d,  $J = 9$ , 2 H, 7.556); 7.556 (d,  $J = 9$ , 2 H, 7.198), 7.198 (d,  $J = 9$ , 2 H, 7.556); 7.519 (d,  $J = 9$ , 2 H, 7.165), 7.165 (d,  $J = 8$ , 2 H, 7.519); 7.490 (d,  $J = 9$ , 2 H, 7.273), 7.273 (d,  $J = 9$ , 2 H, 7.490); 7.474 (d,  $J = 9$ , 2 H, 7.199), 7.199 (d,  $J = 9$ , 2 H, 7.474); 7.465 (d,  $J = 8$ , 2 H, 7.213), 7.213 (d,  $J = 8$ , 2 H, 7.465); 7.463 (d,  $J = 9$ , 2 H, 7.155), 7.155 (d,  $J = 9$ , 2 H, 7.463); 7.402 (d,  $J = 9$ , 2 H, 7.145), 7.145 (d,  $J = 9$ , 2 H, 7.402); 7.404 (d,  $J = 9$ , 2 H, 7.291), 7.291 (d,  $J = 9$ , 2 H, 7.404); 7.404 (d,  $J = 9$ , 2 H, 7.142), 7.142 (d,  $J = 9$ , 2 H, 7.404); 7.386 (d,  $J = 9$ , 2 H, 7.159), 7.159 (d,  $J = 9$ , 2 H, 7.386); 7.381 (d,  $J = 9$ , 2 H, 7.273), 7.273 (d,  $J = 9$ , 2 H, 7.381); 7.254, 7.252 (s, s, 2 H), 7.247 (s, 2 H); two overlapped AB systems. Aliphatic region: 3.000 (s, 3 H), 2.966, 2.964 (s, 3 H), 2.921 (s, 3 H), 2.913, 2.912 (s, 3 H), 2.900 (s, 3 H), 2.877, 2.876 (s, 2 H), 2.862, 2.859 (s, 3 H), 2.852, 2.850 (s, 3 H), 1.228 (s, 9 H), 1.217 (s, 9 H), 1.201 (s, 9 H), 1.194 (s, 9 H), 1.190 (s, 9 H), 1.187 (s, 9 H), 1.179 (s, 9 H), 1.168 (s, 9 H), 1.163 (s, 18 H), 1.159 (s, 9 H).  $^1\text{H}$  NMR (500 MHz, EM =  $-1.50$ , GB = 0.80,  $\text{C}_6\text{D}_6$ , 328 K,  $^1\text{H}\text{--}^1\text{H}$  COSY cross-peaks in aromatic region): Ring A: 8.030 (t,  $J = 2$ , 1 H, 7.837, 7.572), 7.837 (t,  $J = 2$ , 1 H, 8.030, 7.572), 7.572 (t,  $J = 2$ , 1 H, 8.030, 7.837). Ring B: 7.964, 7.960 (t,  $J = 2$ ,  $J = 2$ , 1 H, 7.748, 7.636), 7.748 (t,  $J = 2$ , 1 H, [7.964, 7.960], 7.636), 7.636 (t,  $J = 2$ , 1 H, [7.964, 7.960], 7.748). Ring C: 7.944 (t,  $J = 2$ , 1 H, [7.864, 7.861], 7.837), 7.864, 7.861 (t,  $J = 2$ ,  $J = 2$ , 1 H, 7.944, 7.837), 7.837 (t,  $J = 2$ , 1 H, 7.944, [7.864, 7.861]). Ring D: 7.765, 7.762 (t,  $J = 2$ ,  $J = 2$ , 1 H, 7.678, 7.643), 7.678 (bt,  $J = 2$ , 1 H, [7.765, 7.762], 7.643), 7.643 (t,  $J = 2$ , 1 H, [7.765, 7.762], 7.678). Rings 1–13: 7.554 (d,  $J = 9$ , 2 H, 7.205), 7.205 (d,  $J = 9$ , 2 H, 7.554); 7.522 (d,  $J = 9$ , 2 H, 7.224), 7.224 (d,  $J = 9$ , 2 H, 7.522); 7.519 (d,  $J = 9$ , 2 H, 7.200), 7.200 (d,  $J = 9$ , 2 H, 7.519); 7.504 (d,  $J = 9$ , 2 H, 7.178), 7.178 (d,  $J = 9$ , 2 H, 7.504); 7.459 (d,  $J = 9$ , 2 H, 7.188), 7.188 (d,  $J = 9$ , 2 H, 7.459); 7.448 (d,  $J = 9$ , 2 H, 7.167), 7.167 (d,  $J = 9$ , 2 H, 7.448); 7.446 (d,  $J = 9$ , 2 H, 7.249), 7.249 (d,  $J = 9$ , 2 H, 7.446); 7.436 (d,  $J = 9$ , 2 H, 7.213), 7.213 (d,  $J = 9$ , 2 H, 7.436); 7.408 (d,  $J = 9$ , 2 H, 7.314), 7.314 (d,  $J = 9$ , 2 H, 7.408); 7.376 (d,  $J = 9$ , 2 H, 7.146), 7.146 (d,  $J = 9$ , 2 H, 7.376); 7.368 (d,  $J = 9$ , 2 H, 7.270), 7.270 (d,  $J = 9$ , 2 H, 7.368); 7.364 (d,  $J = 9$ , 2 H, 7.163), 7.163 (d,  $J = 9$ , 2 H, 7.163); 7.258, 7.254 (s, s, 1 H, 1 H), 7.251 (s, 2 H); two overlapped AB systems. Aliphatic region: 2.994 (s, 3 H), 2.964 (s, 3 H), 2.939 (s, 3 H), 2.929, 2.926 (s, 3 H), 2.914 (s, 3 H), 2.893 (s, 3 H), 2.885 (s, 3 H), 2.853, 2.850 (s, 3 H), 1.230 (s, 9 H), 1.219 (s, 9 H), 1.207 (s, 9 H), 1.198 (s, 18 H), 1.192 (s, 9 H), 1.188 (s, 9 H), 1.177 (s, 9 H), 1.174 (s, 9 H), 1.166 (s, 9 H), 1.164 (s, 9 H).  $^{13}\text{C}\{^1\text{H}\}$ DEPT(135 $^{\circ}$ )NMR (125 MHz, EM =  $-1.20$ , GB = 0.80,  $\text{C}_6\text{D}_6$ , 293 K): aromatic quaternary region, expected, 38 resonances; found, 46 resonances at 150.4 (q), 150.2 (q), 150.00 (q), 149.92 (q), 149.86 (q), 149.83 (q), 149.79 (q), 149.70 (q), 149.5 (q), 146.5 (q), 146.3 (q), 145.09 (q), 144.98 (q), 144.86 (q), 144.57 (q), 144.54 (q), 144.3 (q), 144.2 (q), 143.5 (q), 143.39 (q), 143.35 (q), 143.27 (q), 143.25 (q), 143.08 (q), 143.07 (q), 143.03 (q), 143.01 (q), 142.81 (q), 142.77 (q), 142.67 (q), 142.2 (q), 142.10 (q), 142.08 (q), 142.05 (q), 141.93 (q), 141.56 (q), 141.55 (q), 141.28 (q), 141.22 (q), 141.15 (q), 140.97 (q), 140.93 (q), 140.34 (q), 140.31 (q), 121.62 (q), 121.60 (q); aromatic nonquaternary region, expected, 38 resonances; found 29 resonances at 131.5, 131.12, 131.08, 131.00, 130.2, 130.00, 129.97, 129.73, 129.71, 129.68, 129.64, 129.52, 129.49, 129.43, 129.37, 129.2, 128.9, 127.3, 126.17, 126.14, 125.9, 125.39, 125.35, 125.24, 125.20, 125.16, 125.13, 125.07, 125.03; aliphatic region, 88.16 (q), 88.14 (q), 88.11 (q), 87.85 (q), 87.81 (q), 87.65 (q), 87.07 (q), 52.8, 52.59, 52.56, 52.53, 52.49, 52.3, 34.81 (q), 34.80 (q), 34.76 (q), 34.74 (q), 34.71 (q), 31.91, 31.88, 31.86, 31.81, 31.78.

**2-(OMe)<sub>15</sub>**, *t*-BuLi (0.255 mL of a ~1.50 M solution in pentane, 0.383 mmol, Acros) was added to a solution of module **11B** (0.353 g, 0.175 mmol) in THF (2.0 mL) in a heavy-wall Schlenk vessel at  $-78$  °C. After 3 h, the reaction mixture was warmed to  $-20$  °C for 10 min and then recooled to  $-78$  °C. Following addition of ZnCl<sub>2</sub> (0.172 mL of 1.16 M solution in ether, 0.200 mmol), the reaction mixture was allowed to attain ambient temperature for 2 h. The resultant clear orange solution was transferred to a glovebox. Pd(PPh<sub>3</sub>)<sub>4</sub> (6.8 mg, 0.006 mmol) and linker **16** (42.8 mg, 0.088 mmol) were added to the reaction mixture. Subsequently, the reaction mixture was heated in an oil bath at 100 °C for 1.5 days. After extraction with ether, the organic layer was dried over MgSO<sub>4</sub> and concentrated in vacuo to give 351 mg of clear yellow solid. Column chromatography (TLC grade silica gel, 5–10% ether in hexane) gave two fractions with similar *R<sub>f</sub>* on TLC: fraction 1 (higher *R<sub>f</sub>*, 75.5 mg) and fraction 2 (lower *R<sub>f</sub>*, 133.3 mg). Treatment with ether/MeOH of fraction 1 and fraction 2 gave 63.6 mg (17%, white powder, softening to clear solid at 221–223 °C) and 113.9 mg (40%, white powder) of **2-(OMe)<sub>15</sub>** as mixtures of diastereomers. All data are reported below are for fraction 1, following treatment with MeOH/ether. Anal. Calcd for C<sub>300</sub>H<sub>350</sub>O<sub>15</sub>: C, 85.87; H, 8.41. Found: 86.02; H, 8.01. IR (cm<sup>-1</sup>): 1594 (Ar), 1083 (C–O–C). FABMS (ONPOE) wide range scan *m/z* (% RA for *m/z* = 1000–5000): 2066.4 (7.5), 2139.5 (6.5), 2185.8 (8), 4132.2 (57), 4164.7 (100); narrow range scan *m/z* (% RA for *m/z* = 2063–2069) at (*M* – 2OCH<sub>3</sub>)<sup>2+</sup> 2065.0 (63), 2065.5 (77), 2066.0 (100), 2066.5 (85), 2067.0 (76), 2067.5 (45), 2068.0 (40); calcd for C<sub>298</sub>H<sub>344</sub>O<sub>13</sub> at (*M* – 2OCH<sub>3</sub>)<sup>2+</sup> 2065.3 (16), 2065.8 (53), 2066.3 (89), 2066.8 (100), 2067.3 (85), 2067.8 (57), 2068.3 (32); narrow range scan *m/z* (% RA for *m/z* = 2180–2193) at (*M* – C<sub>144</sub>H<sub>167</sub>O<sub>7</sub>)<sup>+</sup> 2184.1 (74), 2185.1 (100), 2186.1 (78), 2187.1 (57), 2188.1 (30); calcd for C<sub>158</sub>H<sub>183</sub>O<sub>8</sub> at (*M* – C<sub>144</sub>H<sub>167</sub>O<sub>7</sub>)<sup>+</sup> 2184.4 (56), 2185.4 (100), 2186.4 (89), 2187.4 (52), 2188.4 (23); narrow range scan *m/z* (% RA for *m/z* = 4156–4176) at (*M* – OCH<sub>3</sub>)<sup>+</sup> 4161.6 (42), 4162.6 (73), 4163.7 (100), 4164.7 (100), 4165.7 (81), 4166.7 (52), 4167.7 (32), 4168.7 (16); calcd for C<sub>299</sub>H<sub>347</sub>O<sub>14</sub> at (*M* – OCH<sub>3</sub>)<sup>+</sup> 4161.6 (16), 4162.7 (52), 4163.7 (88), 4164.7 (100), 4165.7 (84), 4166.7 (58), 4167.7 (32), 4168.7 (16). <sup>1</sup>H NMR (500 MHz, EM =  $-1.95$ , GB = 0.85, C<sub>6</sub>D<sub>6</sub>, 293 K, <sup>1</sup>H–<sup>1</sup>H DQF COSY (600 MHz) cross-peaks in aromatic region): Ring A: 8.093 (bs, 2 H, 7.875, 7.640), 7.875 (bs, 2 H, 8.093, 7.640), 7.640 (bs, 2 H, 8.093, 7.875). Ring B: 7.988 (bs, 2 H, 7.936, 7.819), 7.936 (bs, 2 H, 7.988, 7.819), 7.819 (bs, 2 H, 7.988, 7.936). Ring C: 7.969 (bs, 2 H, 7.761, 7.732), 7.761 (bs, 2 H, 7.969, 7.732), 7.732 (bs, 2 H, 7.969, 7.761). Ring D: 7.792, 7.782 (bs, bs, 2 H, 7.761, 7.701), 7.761 (bs, 2 H, [7.792, 7.782], 7.701), 7.701 (bs, 2 H, [7.792, 7.782], 7.761). Rings 1–23: 7.134–7.603 (m, 92 H). Aliphatic region: normalized to 15 resonances for methoxy groups (45 H), found 11 resonances at 3.002 (bs, 6.11 H), 2.986 (s, 1.31 H), 2.974 (s, 2.04 H), 2.951 (bs, 6.17 H), 2.924 (bs, 6.29 H), 2.896, 2.892, 2.887, 2.882 (s, s, s, s, 12.24 H), 2.866 (bs, 5.54 H), 2.842 (bs, 5.29 H); normalized to 21 resonances for *tert*-butyl groups (189 H), found 11 resonances at 1.246 (bs, 9.87 H), 1.228 (bs, 9.04 H), 1.223 (bs, 12.66 H), 1.200 (bs, 20.30 H), 1.194, 1.187 (bs, bs, 52.00 H), 1.182, 1.177, 1.173 (bs, bs, bs, 38.26 H), 1.167, 1.162 (bs, bs, 46.87 H). <sup>1</sup>H NMR (500 MHz, EM =  $-1.70$ , GB = 0.85, C<sub>6</sub>D<sub>6</sub>, 328 K):  $\delta$  7.10–8.05 (m, 116 H), 2.83–3.03 (m, 45 H), 1.15–1.25 (m, 189 H). <sup>1</sup>H NMR (500 MHz, EM =  $-1.95$ , GB = 0.85, C<sub>6</sub>D<sub>6</sub>, 348 K, <sup>1</sup>H–<sup>1</sup>H DQF COSY (600 MHz) cross-peaks in aromatic region): Ring A: 7.942 (bs, 2 H, [7.766, 7.762], 7.540), 7.766, 7.762 (t, t, *J* = 2, *J* = 2, 2 H, 7.942, 7.540), 7.540 (bs, 2 H, 7.942, [7.766, 7.762]). Ring B: 7.901 (t, *J* = 2, 2 H, 7.846, 7.737), 7.846 (bt, *J* = 2, 2 H, 7.901, 7.737), 7.737 (bs, 2 H, 7.901, 7.846). Ring C: 7.846 (bt, *J* = 2, 2 H, 7.695, 7.613), 7.695 (t, *J* = 2, 2 H, 7.846, 7.613), 7.613 (t, *J* = 2, 2 H, 7.846, 7.695). Ring D: 7.688 (bs, 2 H, 7.637, 7.610), 7.637 (bs, 2 H, 7.688, 7.610), 7.610 (bs, 2 H, 7.688, 7.637). Rings 1–23: 7.109–7.514 (m, 92 H). Aliphatic region: normalized to 15 resonances for methoxy groups (45 H), found 10 resonances at 2.973 (s, 1.37 H), 2.961 (bs, 7.59 H), 2.949 (s, 0.64 H), 2.929 (bs, 6.13 H), 2.918 (bs, 5.93 H), 2.883, 2.880 (s, s, 6.23 H),

2.860 (bs, 11.30 H), 2.848 (s, 3.54 H), 2.842 (s, 2.27); normalized to 21 resonances for *tert*-butyl groups (189 H), found 13 resonances at 1.216 (s, 7.06 H), 1.213 (s, 3.08 H), 1.196 (s, 8.52 H), 1.192, 1.191 (s, s, 13.31 H), 1.177 (bs, 20.76 H), 1.168 (bs, 33.46 H), 1.163, 1.162 (bs, s, 34.49 H), 1.153 (s, 7.25 H), 1.148 (bs, 43.69 H), 1.141, 1.138 (s, s, 17.37 H).

**3-(OMe)<sub>22</sub>**, *t*-BuLi (0.053 mL of a 1.63 M solution in pentane, 0.086 mmol, Acros, twice titrated with *N*-pivaloyl-*o*-toluidine) was added to a solution of module **17** (30.0 mg, 0.0168 mmol) in THF (0.40 mL) in a heavy-wall Schlenk vessel at  $-78$  °C. After 2 h at  $-78$  °C, the reaction mixture was warmed to  $-20$  °C for 10 min and then recooled to  $-78$  °C. Following addition of ZnCl<sub>2</sub> (0.071 mL of 1.06 M solution in ether, 0.076 mmol), the reaction mixture was allowed to attain ambient temperature for 2.5 h. The clear yellow solution was transferred to a glovebox. A solution of Pd(PPh<sub>3</sub>)<sub>4</sub> (0.025 mL of 0.027 M solution in THF, 0.68  $\mu$ mol) and a solution of **15B** (118 mg, 0.050 mmol) were added to the reaction mixture. Subsequently, the reaction mixture was heated in an oil bath at 100 °C for 3 days. After extraction with ether, the organic layer was dried over MgSO<sub>4</sub> and concentrated in vacuo to give a clear solid. Column chromatography (TLC grade silica gel, 5–10% ether in hexane) gave fractions 1 and 2 (F1 and F2 in the order of increasing polarity on silica gel), which were treated with ether/MeOH: F1, **20B-(OMe)<sub>16</sub>** side product, 3.5 mg (3%) of white solid softening at 214 °C, melting at 228–229 °C (clear yellow solid) and becoming clear yellow liquid at 239 °C; F2, **3-(OMe)<sub>22</sub>**, 57.4 mg (56%) of white solid (softening to clear solid at 239–240 °C). From another reaction on the same scale, 34.9 mg (34%) of **3-(OMe)<sub>22</sub>** was obtained from 30.0 mg of **17**.

**3-(OMe)<sub>22</sub>**. Anal. Calcd for C<sub>440</sub>H<sub>508</sub>O<sub>22</sub>: C, 85.95; H, 8.33. Found: 86.31; H, 7.95. IR (cm<sup>-1</sup>): 1594 (Ar), 1082 (C–O–C). FABMS (ONPOE) wide range scan *m/z* (% RA for *m/z* = 2000–8000): 3043 (2.5), 4137 (2.5), 6116.5 (100); narrow range scan *m/z* (% RA for *m/z* = 3039–3048) at (*M* – 2OCH<sub>3</sub>)<sup>2+</sup> 3041.4 (57), 3041.9 (76), 3042.4 (92), 3042.9 (100), 3043.4 (87), 3043.9 (72), 3044.4 (51), 3044.9 (35); calcd for C<sub>438</sub>H<sub>502</sub>O<sub>20</sub> at (*M* – 2OCH<sub>3</sub>)<sup>2+</sup> 3041.4 (20), 3041.9 (48), 3042.4 (80), 3042.9 (100), 3043.4 (100), 3043.9 (82), 3044.4 (59), 3044.9 (36); narrow range scan *m/z* (% RA for *m/z* = 6110–6125) at (*M* – OCH<sub>3</sub>)<sup>+</sup> 6113.9 (42), 6114.9 (70), 6115.9 (100), 6116.9 (100), 6117.9 (96), 6118.9 (74), 6119.9 (54), 6120.9 (34), 6122.0 (21); calcd for C<sub>439</sub>H<sub>505</sub>O<sub>21</sub> at (*M* – OCH<sub>3</sub>)<sup>+</sup> 6113.8 (20), 6114.9 (48), 6115.9 (80), 6116.9 (100), 6117.9 (100), 6118.9 (83), 6119.9 (59), 6120.9 (37), 6121.9 (21). <sup>1</sup>H NMR (500 MHz, EM =  $-1.90$ , GB = 0.90, C<sub>6</sub>D<sub>6</sub>, 293 K, GE): 7.05–8.20 (m, 172 H). Aliphatic region: expected 22 resonances for the methoxy groups, found 26 resonances (66 H) at 3.104, 3.100 (s, s, 2.78 H), 3.010, 3.008 (s, s, 6.28 H), 2.999 (s, 1.46 H), 2.992, 2.990, 2.988 (s, s, s, 2.49 H), 2.980, 2.977, 2.973, 2.968, 2.966 (s, s, s, s, s, 12.29 H), 2.961 (s, 0.97 H), 2.933, 2.928, 2.924, 2.920, 2.915, 2.910, 2.906, 2.902 (bs, s, s, s, bs, s, s, s, 23.64 H), 2.893, 2.889 (s, s, 5.71 H), 2.874 (bs, 5.35 H), 2.852 (bs, 5.03 H); expected 30 resonances for the *tert*-butyl groups, found 14+ resonances at 1.256, 1.252, 1.232, 1.229, 1.225, 1.204, 1.197, 1.191, 1.186, 1.179, 1.168, 1.146–1.164, 1.138, 1.135, 1.132 (14 singlets and 1 multiplet, 270 H). <sup>1</sup>H NMR (500 MHz, EM =  $-1.40$ , GB = 0.90, C<sub>6</sub>D<sub>6</sub>, 328 K, GE): 7.05–8.15 (m, 172 H), 2.80–3.15 (19 singlets, 66 H), 1.10–1.35 (18 singlets and 1 multiplet, 270 H). <sup>1</sup>H NMR (500 MHz, EM =  $-1.20$ , GB = 0.90, C<sub>6</sub>D<sub>6</sub>, 348 K, <sup>1</sup>H–<sup>1</sup>H COSY cross-peaks in aromatic region): Ring A: 8.061 (br, 1 H, 7.984 (weak)), 8.009 (br, 1 H), 7.984 (br, 1 H, 8.061 (weak)); cross-peaks are missing. Ring B: 7.980 (br, 1 H, [7.840, 7.837], 7.403), 7.840, 7.837 (t, t, *J* = 2, *J* = 2, 1 H, 7.980, 7.403), 7.403 (br, 1 H, 7.980, [7.840, 7.837]). Rings C/D (tentative assignment): 7.772 (br), 7.706 (br), 7.699 (br), 7.606 (br); peaks and cross-peaks are missing. Ring E, E': 7.989 (br, 2 H, [7.811, 7.808], 7.585), 7.811, 7.808 (t, t, *J* = 2, *J* = 2, 2 H, 7.989, 7.585), 7.585 (t, *J* = 2, 2 H, 7.989, [7.811, 7.808]). Ring F, F': 7.946 (bs, 2 H, [7.890, 7.886], [7.786, 7.782]), 7.890, 7.886 (t, t, *J* = 2, *J* = 2, 2 H, 7.946, [7.786, 7.782]), 7.786, 7.782 (t, t, *J* = 2, *J* = 2, 2 H, 7.946, [7.890,

7.886]). Ring G, G': 7.899, 7.895 (t, t,  $J = 2$ ,  $J = 2$ , 2 H, 7.741, 7.662), 7.741 (t,  $J = 2$ , 2 H, [7.899, 7.895], 7.662), 7.662 (t,  $J = 2$ , 2 H, [7.899, 7.895], 7.741). Ring H, H': 7.732 (br, 2 H, 7.683, [7.658, 7.654]), 7.683 (br, 2 H, 7.732, [7.658, 7.654]), 7.658, 7.654 (t, t,  $J = 2$ ,  $J = 2$ , 2 H, 7.732, 7.683). Rings 1–34: 7.16–7.60 (m, 136 H). Aliphatic region: expected 22 resonances for the methoxy groups, found 21 resolved resonances (66 H) at 3.106 (s, 2.71 H), 3.026 (s, 0.87 H), 3.020 (s, 0.92 H), 3.015 (s, 0.85 H), 3.010 (s, 0.96 H), 3.004 (s, 6.75 H), 2.996, 2.994 (s, s, 1.63 H), 2.986 (s, 0.93 H), 2.978, 2.972, 2.967, 2.961 (s, s, s, s, 18.07 H), 2.946, 2.943 (s, bs, 5.94 H), 2.926, 2.924, 2.920 (s, s, s, 9.03 H), 2.903 (bs, 11.54 H), 2.890, 2.885 (s, s, 5.80 H); expected 30 resonances for the *tert*-butyl groups, found 17 resonances at 1.263, 1.261, 1.258, 1.254, 1.236, 1.232, 1.216, 1.209, 1.207, 1.203, 1.201, 1.191, 1.187, 1.179, 1.175, 1.156, 1.154 (17 singlets, 270 H).

**4-(OMe)<sub>36</sub>**, *t*-BuLi (0.041 mL of a 1.70 M solution in pentane, 0.070 mmol, Acros, twice titrated with *N*-pivaloyl-*o*-toluidine) was added to a solution of **18** (9.4 mg, 0.0071 mmol) in THF (0.30 mL) in a heavy-wall Schlenk vessel at  $-78$  °C. After 2 h at  $-78$  °C, the reaction mixture was warmed to  $-20$  °C for 10 min and then recooled to  $-78$  °C. Following addition of ZnCl<sub>2</sub> (0.030 mL of 1.13 M solution in ether, 0.034 mmol), the reaction mixture was allowed to attain ambient temperature for 3.5 h. The resultant turbid gel was transferred to a glovebox. A solution of Pd(PPh<sub>3</sub>)<sub>4</sub> (0.050 mL of 0.014 M solution in THF, 0.00070 mmol) and a solution of racemic **15A** (102.0 mg, 0.044 mmol) were added to the reaction mixture. Subsequently, the reaction mixture was heated in an oil bath at 100 °C for 2.5 days. After extraction with ether, the organic layer was dried over MgSO<sub>4</sub> and concentrated in vacuo to give a clear solid. Analogous procedure was implemented for the other two reactions. The isolated yields from the reactions I, II, and III were 7%, 22%, 32%, respectively. For mixtures of compounds, the relative amounts were determined with <sup>1</sup>H NMR (500 MHz, C<sub>6</sub>D<sub>6</sub>) spectroscopy. The purification protocols for each reaction were as follows.

**Reaction I.** Column chromatography (TLC grade silica gel, 5–10% ether in hexane) gave 21.9 mg of clear glass; FABMS (% RA *form/z* = 3000–12000) 10021 (8), 7761 (15), 4979 (8), 4492 (100), 3865 (10) and <sup>1</sup>H NMR spectroscopy showed a mixture of **4-(OMe)<sub>36</sub>**, **19-(OMe)<sub>28</sub>**, and **20A-(OMe)<sub>16</sub>** (1:2:2.5). PTLC (activated silica, 8% ether in hexane, developed 3–4 times) gave two fractions (in order of increasing polarity). Fraction 1 (less polar, 4.7 mg) was primarily **19-(OMe)<sub>28</sub>** with a contamination of **20A-(OMe)<sub>16</sub>(OH)**. Additional PTLC (activated silica, 10% ether in hexane), using 3.9 mg of fraction 1, gave <0.5 mg of **19-(OMe)<sub>28</sub>**. Fraction 2 (7.6 mg) was treated with MeOH/ether to give 5.2 mg (7%) of clear glass. FABMS (% RA for *m/z* = 2500–12600): 10019 (20), 7761 (<5), 4994 (30), 4478 (100). A portion of Fraction 2 was filtered through cotton plug. FABMS (% RA for *m/z* = 3500–11000): 10021 (20), 7762 (<5), 4995 (20), 4479 (100). Overall yield **4-(OMe)<sub>36</sub>** is 5.2 mg, 7%, based on Fraction 2.

**Reaction II.** Column chromatography (TLC grade silica gel, 5–10% ether in hexane) was carried out twice to produce four fractions. Treatment with MeOH/ether gave fractions 1–4 (in order of increasing polarity). Fraction 1 (2.9 mg) was a mixture of **4-(OMe)<sub>36</sub>**, **20A-(OMe)<sub>16</sub>**, **19-(OMe)<sub>28</sub>**, and unknown impurity. FABMS (% RA for *m/z* = 2500–12000): 9992 (10), 7763 (15), 5499 (15), 4995 (<3), 4493 (15). Fraction 2 (10.6 mg) was a mixture of **4-(OMe)<sub>36</sub>**, **19-(OMe)<sub>28</sub>**, and unknown impurity. FABMS (% RA for *m/z* = 2500–12000): 10024 (60), 7762 (50), 5500 (15), 4996 (40), 3866 (25). Fraction 3 (12.1 mg) was a mixture of **4-(OMe)<sub>36</sub>** and **19-(OMe)<sub>28</sub>** (10:1). FABMS (% RA for *m/z* = 2500–12000): 10022 (100), 7762 (60), 4996 (65), 3865 (20). Fraction 4 (14.6 mg) was a mixture of **4-(OMe)<sub>36</sub>** and **19-(OMe)<sub>28</sub>** (10:1). FABMS (% RA for *m/z* = 2500–12000): 10022 (100), 7762 (35), 4996 (55), 3865 (15). Overall yield **4-(OMe)<sub>36</sub>** was 26.7 mg, 22%, based on Fractions 3 and 4.

**Reaction III.** Column chromatography (TLC grade silica gel, 5–10% ether in hexane), followed by treatment with ether/MeOH, gave three isolated fractions (in the order of increasing polarity on silica

gel) as clear glasses. Fraction 1 was side product **20A-(OMe)<sub>16</sub>** (white solid, 8.0 mg, 8%). Fraction 2 (9.0 mg) was **4-(OMe)<sub>36</sub>** and **19-(OMe)<sub>28</sub>** (10:1). Fraction 3 (13.7 mg) was **4-(OMe)<sub>36</sub>** and **19-(OMe)<sub>28</sub>** (10:1). FABMS (% RA for *m/z* = 2500–12000): 10022 (100), 7762 (45), 4995 (85), 3865 (25). Overall yield **4-(OMe)<sub>36</sub>** was 22.7 mg, 32%, based on Fractions 2 and 3.

**(OMe)<sub>36</sub>**, White solid (softening to clear solid at 272–274 °C). IR (cm<sup>-1</sup>): 1594 (Ar), 1082 (C–O–C). FABMS (ONPOE) wide range scan *m/z* (% RA for *m/z* = 3000–12000) at (*M* – OCH<sub>3</sub>)<sup>+</sup>: 10021.6 (100), at (*M* – 2OCH<sub>3</sub>)<sup>2+</sup> 4995.3 (85). Narrow range scans *m/z* (% RA for *m/z* = 10005–10040, 9880–11000) at (*M* – OCH<sub>3</sub>)<sup>+</sup> for two different samples: 10021.5 (100) and 10021.9 (100); calcd for C<sub>719</sub>H<sub>821</sub>O<sub>35</sub> at (*M* – OCH<sub>3</sub>)<sup>+</sup> av mass = 10023.45, peak maximum mass = 10023.04. <sup>1</sup>H NMR (500 MHz, EM =  $-1.90$ , GB = 0.50, C<sub>6</sub>D<sub>6</sub>, 293 K, <sup>1</sup>H–<sup>1</sup>H DQF–COSY cross-peaks in aromatic region). Rings A, A': 8.079 (bs, 8 H, 7.983, 7.513), 7.983 (bs, 8 H, 8.079, 7.513), 7.513 (bs, 8 H, 8.079, 7.983). Rings B and C: 7.943 (bs, 8 H, 7.796), 7.796 (bs, 4 H, 7.943); 7.883 (bs, 4 H, 7.637), 7.637 (bs, 8 H, 7.883). Rings 1,1'–5,5': 7.575 (d,  $J = 9$ , 16 H, 7.253), 7.253 (d,  $J = 9$ , 16 H, 7.575); 7.557, 7.561 (d,  $J = 9$ , 16 H, 7.197, 7.200), 7.197, 7.200 (d,  $J = 9$ , 16 H, 7.557, 7.561); 7.487 (d,  $J = 9$ , 16 H, 7.213), 7.213 (d,  $J = 9$ , 16 H, 7.487); 7.439 (d,  $J = 8$ , 16 H, 7.213), 7.213 (d,  $J = 9$ , 16 H, 7.439); 7.378 (d,  $J = 9$ , 16 H, 7.149), 7.149 (d,  $J = 9$ , 16 H, 7.378). Rings 6–9: 7.637 (bs, 8 H, 7.231), 7.231 (bs, 8 H, 7.637); 7.477 (d,  $J = 8$ , 8 H, 7.295), 7.295 (d,  $J = 9$ , 8 H, 7.477); 7.415 (d,  $J = 9$ , 8 H, 7.356), 7.356 (d,  $J = 9$ , 8 H, 7.415); 7.378 (d,  $J = 9$ , 8 H, 7.149), 7.149 (d,  $J = 9$ , 8 H, 7.378) (tentative assignment). Aliphatic region: 3.161 (s, 12 H), 2.986 (s, 12 H), 2.982 (s, 12 H), 2.973 (s, 12 H), 2.912 (s, 24 H), 2.893 (s, 12 H), 2.851 (s, 12 H), 2.848 (s, 12 H), 1.253, 1.250 (s, s, 36 H), 1.210 (s, 72 H), 1.196 (s, 144 H), 1.181 (s, 72 H), 1.165 (s, 72 H), 1.053 (m, 36 H). <sup>1</sup>H NMR (500 MHz, EM =  $-1.30$ , GB = 0.90, C<sub>6</sub>D<sub>6</sub>, 328 K, <sup>1</sup>H–<sup>1</sup>H COSY cross-peaks in aromatic region): Rings A, A': 8.019, 8.016 (bs, bs, 8 H, 7.912, 7.480), 7.912 (bs, 8 H, [8.019, 8.016], 7.480), 7.480 (bs, 8 H, [8.019, 8.016], 7.912). Rings B and C: 7.944 (d,  $J = 2$ , 8 H, 7.704), 7.704 (bs, 4 H, 7.944); 7.835 (t,  $J = 2$ , 4 H, 7.597), 7.597 (d,  $J = 2$ , 8 H, 7.835). Ring D: 8.07 (bs, 4 H), 7.95 (bs, 8 H). Rings 1–9: 7.15–7.55 (m, 224 H). Aliphatic region: 3.172 (bs, 12 H), 2.991, 2.988 (s,s, 36 H), 2.937 (s, 24 H), 2.889 (s, 12 H), 2.876, 2.873 (s, s, 24 H), 1.254 (s, 36 H), 1.216 (s, 72 H), 1.208 (s, 72 H), 1.200 (s, 72 H), 1.190 (s, 72 H), 1.179 (s, 72 H), 1.068 (m, 36 H). <sup>1</sup>H NMR (500 MHz, EM =  $-1.19$ , GB = 0.48, C<sub>6</sub>D<sub>6</sub>, 348 K, <sup>1</sup>H–<sup>1</sup>H DQF–COSY cross-peaks in aromatic region): Rings A, A': 7.983, 7.979 (t, t,  $J = 2$ ,  $J = 2$ , 8 H, 7.873, 7.462), 7.873 (t,  $J = 2$ , 8 H, [7.983, 7.979], 7.462), 7.462 (t,  $J = 2$ , 8 H, [7.983, 7.979], 7.873). Rings B and C: 7.935 (d,  $J = 2$ , 8 H, 7.661), 7.661 (bt,  $J = 2$ , 4 H, 7.935); 7.810 (t,  $J = 2$ , 4 H, 7.572), 7.572 (d,  $J = 2$ , 8 H, 7.810). Rings D: 8.015 (bs, 4 H), 7.936 (bs, 8 H). Rings 1,1'–5,5': 7.516 (d,  $J = 9$ , 16 H, 7.207), 7.207 (d,  $J = 8$ , 16 H, 7.516); 7.516 (d,  $J = 9$ , 16 H, 7.240), 7.240 (d,  $J = 9$ , 16 H, 7.516); 7.447 (d,  $J = 9$ , 16 H, 7.223), 7.223 (d,  $J = 8$ , 16 H, 7.447); 7.399 (d,  $J = 9$ , 16 H, 7.207), 7.207 (d,  $J = 8$ , 16 H, 7.399); 7.348 (d,  $J = 8$ , 16 H, 7.163), 7.163 (d,  $J = 9$ , 16 H, 7.348). Rings 6–9: 7.594 (bd,  $J \approx 9$ , 8 H, 7.223), 7.223 (d,  $J = 8$ , 8 H, 7.594); 7.467 (d,  $J = 8$ , 8 H, 7.294), 7.294 (d,  $J = 9$ , 8 H, 7.467); 7.457 (d,  $J = 8$ , 8 H, 7.410), 7.410 (d,  $J = 8$ , 8 H, 7.457); 7.443 (s, 8 H), 7.438 (s, 8 H) as AB system. Aliphatic region: 3.176 (bs, 12 H), 3.005 (s, 12 H), 2.995 (s, 12 H), 2.992 (s, 12 H), 2.949 (s, 24 H), 2.888 (s, 36 H), 1.258 (s, 36 H), 1.220 (s, 72 H), 1.215 (bs, 72 H), 1.206 (bs, 72 H), 1.196 (s, 72 H), 1.188 (s, 72 H), 1.082 (m, 36 H). <sup>13</sup>C NMR (125 MHz, C<sub>6</sub>D<sub>6</sub>, 348 K): aromatic quaternary region, expected, 27 resonances; found, 11 resonances at 150.22 (q), 150.14 (q), 150.11 (q), 150.04 (q), 149.93 (q), 149.89, 143.8 (q), 143.5 (q), 143.2 (q), 142.8 (q), 142.7 (q); <sup>1</sup>H–<sup>13</sup>C NMR (500 MHz, C<sub>6</sub>D<sub>6</sub>, <sup>1</sup>H–<sup>13</sup>C HMQC–GS cross-peaks in aromatic nonquaternary region, 348 K), expected, 27 resonances; found 26 resonances at 130.3 (7.465, not assigned), 130.2 (7.416, 7.410, rings 6–9), 130.0 (7.434, 7.443 or 7.438, rings 6–9), 129.92 (7.381, not

assigned), 129.88 (7.451, 7.447, rings 1,1'-5,5'), 129.81 (7.399, 7.399, rings 1,1'-5,5'), 129.66 (7.572, 7.572, rings B or C), 129.63 (7.863, 7.873, rings A,A'), 129.56 (7.522, 7.516, rings 1,1'-5,5'), 129.45 (7.468, 7.467, rings 6-9), 129.45 (7.468, 7.462, rings A,A'), 129.37 (7.348, 7.348, rings 1,1'-5,5'), 129.15 (7.516, 7.516, rings 1,1'-5,5'), 129.11 (7.973, 7.983 and 7.979, rings A,A'), 128.4 (7.809, 7.810, rings B or C), 127.3 (7.452, 7.457, rings 6-9), 127.2 (7.434, 7.443 or 7.438, rings 6-9), 126.4 (7.933, 7.935, rings B or C), 125.26 (7.282, 7.294, rings 6-9), 125.19 (7.205, 7.207, rings 1,1'-5,5'), 125.19 (7.205, 7.207, rings 1,1'-5,5'), 125.13 (7.227, 7.223, rings 1,1'-5,5'), 125.13 (7.227, 7.223, rings 6-9), 125.06 (7.292, not assigned), 125.045 (7.25 (sh), 7.240, rings 1,1'-5,5'), 125.04 (7.148, 7.163, rings 1,1'-5,5'); aliphatic region, 88.4 (q), 88.3 (q), 88.0 (q), 52.75, 52.67, 52.62, 52.53, 34.88 (q), 34.84 (q), 34.82 (q), 34.81 (q), 31.93, 31.90. <sup>13</sup>C NMR (125 MHz, C<sub>6</sub>D<sub>6</sub>, 298 K): aromatic quaternary region, expected, 27 resonances; found, 23 resonances at 150.06 (q), 149.97 (q), 149.8 (q), 149.72 (q), 149.67 (q), 146.2 (q), 144.8 (q), 144.6 (q), 143.9 (q), 143.8 (q), 143.5 (q), 143.4 (q), 143.17 (q), 143.15 (q), 142.8 (q), 142.7 (q), 142.5 (q), 142.4 (q), 141.6 (q), 141.2 (q), 140.5 (q), 140.4 (q), 140.3 (q); aromatic nonquaternary region, expected, 27 resonances; found 16 resonances at 130.21, 130.12, 130.0, 129.6, 129.4, 129.3, 129.1, 128.9, 127.9, 127.4, 127.1, 126.4, 125.9, 125.3, 125.2, 125.0; aliphatic region, 90.1 (q), 88.2 (q), 88.1 (q), 87.8 (q), 87.6 (q), 87.2 (q), 52.60, 52.51, 52.47, 52.42, 34.80 (q), 34.78 (q), 34.74 (q), 31.88, 31.85.

**20A-(OMe)<sub>16</sub>.** Softening at 130 °C and melting at 154–156 °C. IR (cm<sup>-1</sup>): 1594 (Ar), 1082 (C–O–C). FABMS (3-NBA) wide range scan *m/z* (% RA for *m/z* = 2000–8000): for (*M* – 2OCH<sub>3</sub>)<sup>2+</sup> 2231.5 (16), 4493.1 (100). Narrow range scan *m/z* (% RA for *m/z* = 4486–4500) at (*M* – OCH<sub>3</sub>)<sup>+</sup> 4490.0 (34), 4491.0 (64), 4492.0 (91), 4493.0 (100), 4494.0 (85), 4495.0 (58), 4496.0 (36), 4497.0 (18); calcd for C<sub>323</sub>H<sub>371</sub>O<sub>15</sub> at (*M* – OCH<sub>3</sub>)<sup>+</sup> 4489.8 (12), 4490.8 (44), 4491.8 (82), 4492.8 (100), 4493.8 (92), 4494.8 (68), 4495.9 (41), 4496.9 (22). <sup>1</sup>H NMR (600 MHz, EM = –1.50, GB = 0.50, C<sub>6</sub>D<sub>6</sub>, 293 K, <sup>1</sup>H–<sup>1</sup>H DQF COSY cross-peaks in aromatic region): Rings A, A': 8.098 (br, 4 H, 7.989, 7.508), 7.989 (br, 4 H, 8.098, 7.508), 7.508 (br, 4 H, 8.098, 7.989). Rings B and C: 7.935 (br, 4 H, 7.819), 7.819 (br, 2 H, 7.935); 7.890 (br, 2 H, 7.641), 7.641 (br, 4 H, 7.890). Rings 1,1'-5,5': 7.587 (d, *J* = 8, 8 H, 7.253), 7.253 (d, *J* = 9, 8 H, 7.587); 7.561 (d, *J* = 8, 8 H, 7.190), 7.190 (d, *J* = 8, 8 H, 7.561); 7.496 (d, *J* = 9, 8 H, 7.217), 7.217 (d, *J* = 8, 8 H, 7.496); 7.448 (d, *J* = 8, 8 H, 7.213), 7.213 (d, *J* = 8, 8 H, 7.448); 7.382 (d, *J* = 8, 8 H, 7.149), 7.149 (d, *J* = 8, 8 H, 7.382). Rings 6–8: 7.608 (d, *J* = 8, 4 H, 7.504), 7.504 (d, *J* = 8, 4 H, 7.608); 7.533 (d, *J* = 8, 4 H, 7.289), 7.289 (d, *J* = 8, 4 H, 7.533); 7.426, 7.420 (s, s, 8 H) AB system; a small singlet at 7.405 is consistent with *J* = 9 Hz coupling constant. Aliphatic region: 3.028 (s, 6 H), 2.982 (bs, 12 H), 2.911 (bs, 12 H), 2.889 (bs, 6 H), 2.850, 2.846, 2.845 (bs, s, s, 12 H), 1.221 (bs, 18 H), 1.207 (bs, 36 H), 1.194 (bs, 72 H), 1.178, 1.177 (bs, s, 36 H), 1.159 (bs, 36 H). <sup>1</sup>H NMR (500 MHz, EM = –0.80, GB = 0.50, C<sub>6</sub>D<sub>6</sub>, 328 K): 8.029, 8.025 (t, t, *J* = 2, *J* = 2, 4 H), 7.936 (d, *J* = 2, 4 H), 7.911 (t, *J* = 2, 4 H), 7.840 (t, *J* = 2, 2 H), 7.719 (bt, *J* = 2, 2 H), 7.605 (d, *J* = 9, 4 H), 7.592 (d, *J* = 2, 4 H), 7.44–7.55 (m, 54 H), 7.420 (d, *J* = 9, 8 H), 7.359 (d, *J* = 9, 8 H), 7.296, 7.294 (d, d, *J* = 9, *J* = 9, 4 H), 7.19–7.25 (m, 24 H), 7.158 (d, *J* = 9, 8 H), 3.050 (s, 6 H), 3.992, 3.990 (s, s, 12 H), 2.939 (bs, 12 H), 2.886 (s, 6 H), 2.879, 2.876 (s, s, 12 H), 1.234, 1.232 (s, s, 18 H), 1.214 (s, 36 H), 1.204, 1.203 (s, 72 H), 1.190 (s, 36 H), 1.177 (s, 36 H). <sup>1</sup>H NMR (500 MHz, EM = –0.7, GB = 0.50, C<sub>6</sub>D<sub>6</sub>, 348 K, <sup>1</sup>H–<sup>1</sup>H DQF COSY cross-peaks in aromatic region): Rings A, A': 7.982, 7.979 (t, t, *J* = 2, *J* = 2, 4 H, 7.989, 7.448), 7.865 (t, *J* = 2, 4 H, [7.982, 7.979], 7.448), 7.448 (t, *J* = 2, 4 H, [7.982, 7.979], 7.865). Rings B and C: 7.922 (d, *J* = 2, 4 H, 7.674), 7.674 (t, *J* = 2, 2 H, 7.922); 7.812 (t, *J* = 2, 2 H, 7.563), 7.563 (d, *J* = 2, 4 H, 7.812). Rings 1,1'-5,5': 7.512 (d, *J* = 9, 8 H, 7.203), 7.203 (d, *J* = 9, 8 H, 7.512); 7.512 (d, *J* = 9, 8 H, 7.236), 7.236 (d, *J* = 8, 8 H, 7.512); 7.444 (d, *J* = 9, 8 H, 7.220), 7.220 (d, *J* = 9, 8 H, 7.444); 7.398 (d, *J* = 9, 8 H, 7.205), 7.205 (d, *J* = 9, 8 H, 7.398); 7.342 (d, *J* = 9, 8 H,

7.159), 7.159 (d, *J* = 9, 8 H, 7.342). Rings 6–8: 7.596 (d, *J* = 7, 4 H, 7.496), 7.496 (d, *J* = 7, 4 H, 7.596); 7.512 (d, *J* = 9, 4 H, [7.294, 7.292]), 7.294, 7.292 (d, d, *J* = 9, *J* = 9, 4 H, 7.512); 7.476, 7.467 (s, s, 8 H) AB system; a small singlet at 7.494 is consistent with *J* = 9 Hz coupling constant. Aliphatic region: 3.059 (s, 6 H), 2.993, 2.992 (s, s, 12 H), 2.949 (bs, 12 H), 2.889, 2.887 (s, s, 12 H), 2.881 (s, 6 H), 1.237, 1.236 (s, s, 18 H), 1.216 (s, 36 H), 1.209 (s, 36 H), 1.206 (s, 36 H), 1.194 (s, 36 H), 1.184 (s, 36 H).

**SQUID Magnetometry.** Quantum Design (San Diego, CA) MPMS5S (with continuous temperature control) was used. The sample tubes were inserted to the magnetometer at low temperature under helium atmosphere and then evacuated and purged with helium, as described elsewhere.<sup>1</sup> Following the measurements, sample tubes were stored at ambient temperature for several weeks, until they were diamagnetic in the 1.8–150 K range. Such samples were carefully reinserted to the magnetometer, with the sample chamber at 200 or 290 K. Then, the temperature was slowly lowered to 10 K to condense the solvent and to freeze the sample. The identical sequence of measurements, as the original sample, was carried out. The resultant data were used for the point-by-point correction for diamagnetism.

**Numerical Curve Fitting for Magnetic Data.** The SigmaPlot for Windows software package was used for numerical curve fitting. The reliability of a fit was measured by the parameter dependence, which was defined as follows: *dependence* = 1 – ((variance of the parameter, other parameters constant)/(variance of the parameter, other parameters changing)). Values close to 1 indicated overparametrized fit.

*M* vs *H* data at low temperatures (*T* = 1.8, 2.5, 3.5, 5, 10 K) were numerically fit as *M* vs *H/T*, using eqs 1 and 2, as described in the text. (More detailed version of eq 2 is described in the Supporting Information, i.e., eqs 1s–7s, and Table 7s.) Except for the results for pentadecaradical **2** (Table 1), the numerical fits were weighed with magnetization (*M*); such weighing was especially useful for the most spin-polydisperse samples (and relatively high values of *S<sub>s</sub>*), improving the agreement between the fit and the experimental data in the *H/T* range near the paramagnetic saturation.

**Acknowledgment.** This research was supported by the National Science Foundation (Chemistry Division) and the National Center for Neutron Research (beam time on NG3, grants no. 1781 and no. 2471). We thank Drs. Maren Pink and Victor G. Young, Jr. of the X-ray Crystallographic Laboratory at the University of Minnesota for the structure determination of compound **7E**. We thank Drs. Ronald Cerny and Richard Schoemaker for their help with mass spectral analyses and NMR spectral determinations. We thank Dr. S. R. Desai for preparation of selected synthetic intermediates. We thank Drs. Paul Butler and Sung-Min Choi for technical assistance with the small angle neutron scattering experiments.

**Supporting Information Available:** Experimental section (materials and special procedures); NMR spectroscopy and other analyses; small angle neutron scattering; numerical curve fitting of magnetic data to the percolation model (eqs 1s–7s, Table 7s, Figure 11s); synthesis and/or characterization of compounds **5**, **7**, **8**, **9**, **10A–10C**, **12**, **13**, **14**, **19-(OMe)<sub>28</sub>**, and **20B-(OMe)<sub>16</sub>**; Tables 1s–5s (summary of NMR data for **10A–10C**, modules **11A–11D**, and modules-with-linkers **15A** and **15B**); Table 6s (summary of GPC/MALS data); Figures 1s–10s (selected NMR spectra and summary plot of GPC/MALS data). This material is available free of charge via the Internet at <http://pubs.acs.org>.

JA031549B